AMERICAN SOCIETY FOR MICROBIOLOGY | Applied and Environmental Microbiology

Spotlight Selection | Environmental Microbiology | Full-Length Text

AoMedA has a complex regulatory relationship with AoBrlA, AoAbaA, and AoWetA in conidiation, trap formation, and secondary metabolism in the nematode-trapping fungus *Arthrobotrys oligospora*

Na Bai,[1,2] Meihua Xie,[3] Qianqian Liu,[1,2] Yingmei Zhu,[1,2] Xuewei Yang,[1,2] Ke-Qin Zhang,[1,2] Jinkui Yang[1,2]

AUTHOR AFFILIATIONS See affiliation list on p. 21.

ABSTRACT The asexual sporulation of filamentous fungi is an important mechanism for their reproduction, survival, and pathogenicity. In *Aspergillus* and several filamentous fungi, BrlA, AbaA, and WetA are the key elements of a central regulatory pathway controlling conidiation, and MedA is a developmental modifier that regulates temporal expression of central regulatory genes; however, their roles are largely unknown in nematode-trapping (NT) fungi. *Arthrobotrys oligospora* is a representative NT fungus, which can capture nematodes by producing adhesive networks (traps). Here, we characterized the function of AoMedA and three central developmental regulators (AoBrlA, AoAbaA, and AoWetA) in *A. oligospora* by gene disruption, phenotypic comparison, and multi-omics analyses, as these regulators are required for conidiation and play divergent roles in mycelial development, trap formation, lipid droplet accumulation, vacuole assembly, and secondary metabolism. A combined analysis of phenotypic traits and transcriptome showed that AoMedA and AoWetA are involved in the regulation of peroxisome, endocytosis, and autophagy. Moreover, yeast one-hybrid analysis showed that AoBrlA can regulate AoMedA, AoAbaA, and AoWetA, whereas AoMedA and AoAbaA can regulate AoWetA. Our results highlight the important roles of AoMedA, AoBrlA, AoAbaA, and AoWetA in conidiation, mycelia development, trap formation, and pathogenicity of *A. oligospora* and provide a basis for elucidating the relationship between conidiation and trap formation of NT fungi.

IMPORTANCE Conidiation is the most common reproductive mode for many filamentous fungi and plays an essential role in the pathogenicity of fungal pathogens. Nematode-trapping (NT) fungi are a special group of filamentous fungi owing to their innate abilities to capture and digest nematodes by producing traps (trapping devices). Sporulation plays an important role in the growth and reproduction of NT fungi, and conidia are the basic components of biocontrol reagents for controlling diseases caused by plant-parasitic nematodes. *Arthrobotrys oligospora* is a well-known NT fungus and is a routinely used model fungus for probing the interaction between fungi and nematodes. In this study, the functions of four key regulators (AoMedA, AoBrlA, AoAbaA, and AoWetA) involved in conidiation were characterized in *A. oligospora*. A complex interaction between AoMedA and three central regulators was noted; these regulators are required for conidiation and trap formation and play a pleiotropic role in multiple intracellular activities. Our study first revealed the role of AoMedA and three central regulators in conidiation, trap formation, and pathogenicity of *A. oligospora*, which contributed to elucidating the regulatory mechanism of conidiation in NT fungi and helped in developing effective reagents for biocontrol of nematodes.

Editor Yvonne Nygård, Chalmers University of Technology, Gothenburg, Sweden

Address correspondence to Jinkui Yang, jinkui960@ynu.edu.cn.

The authors declare no conflict of interest.

See the funding table on p. 21.

Received 12 June 2023
Accepted 13 July 2023
Published 1 September 2023

KEYWORDS *Arthrobotrys oligospora*, developmental regulator, conidiation, trap formation, secondary metabolism

Filamentous fungi are organisms with diversified reproduction strategies, with most of their lifecycle being spent on asexual reproduction (1). Asexual spores are critical in the lifecycle of most filamentous fungi (2), and conidia are the main type of asexual spores, which occur after a period of vegetative growth when the specialized aerial hyphae differentiate into conidia (3). Conidiation in *Aspergillus* species, particularly in the model organism *Aspergillus nidulans*, has been studied extensively. Conidiation of filamentous fungi involves many aspects, including spatial and temporal regulation of gene expression, specialized cell differentiation, intracellular/intercellular communication, and response to environmental factors (4). BrlA activates a central regulatory pathway to control the temporal and spatial expression of conidiation-specific genes (5), and BrlA, AbaA, and WetA are the key core regulatory proteins, and MedA is identified as a temporal modifier of the expression of these core conidiation proteins (6).

The central development pathway consists of BrlA, AbaA, and WetA which are indispensable for sporulation in the model fungus *A. nidulans* and other *Aspergillus* species (7). MedA expression begins after the induction of conidiation and persists throughout the asexual cycle (8). It is a developmental modifier necessary for correct conidial morphogenesis through spatial and temporal regulation of *brlA* and *abaA* expression (9). The regulatory sequence for central regulatory components is BrlA→ AbaA→ WetA, and they play a crucial role in asexual development. Central regulatory components are functionally conserved in conidiogenesis in *A. nidulans* (10), *A. fumigatus* (11), *Penicillium decumbens* (12), and *P. digitatum* (13). In plant-pathogenic fungus *Magnaporthe grisea* (syn. *M. oryzae*), ACR1 is the ortholog of MedA, which is required for conidiophore architecture and pathogenicity and infection-related morphogenesis (14, 15). Recently, the role of central regulatory components was also revealed in several entomopathogenic fungi. For example, BrlA and AbaA are important regulators of conidiation, insect pathogenicity, and dimorphism transformation in *Beauveria bassiana* (16), and WetA is dispensable for conidiation as well as conidial maturation and virulence (17). In addition, as conidia are diffusive propagules, they are essential in disease transmission and are also effective components of fungal insecticides; hence, conidia have vital significance in pathogenicity (18).

Most fungal lifestyle transitions are complex. Among pathogenic fungi, nematode-trapping (NT) fungi are unique as their hyphae can form ingenious structures (traps) to capture nematodes when sensing prey, and the formation of traps is the key indicator of their lifestyle transition from saprophytes to predators; thus, they are a good model for studying the pathogenesis and adaptation mechanism of fungi (19, 20). *Arthrobotrys oligospora* is a typical NT fungus that can complete its reproduction asexually by producing abundant conidia and adhesive three-dimensional networks for nematode predation; therefore, it has been widely used in studying the interactions between fungi and nematodes (21, 22). Recent studies have shown that several signaling proteins, including regulators of G-protein (23, 24), mitogen-activated protein kinases (25–28), and small GTPases (29–31), are involved in conidiation in *A. oligospora*. In addition, autophagy-related proteins (32, 33) and peroxisome biogenesis proteins (34, 35) play an important role in the interaction between fungi and nematodes and regulating conidiation. In our previous study, two velvet proteins VosA and VelB involved in conidiation were identified in *A. oligospora*. VelB is essential for conidiation, trap formation, and pathogenicity, whereas VosA plays a minor role in the regulation of conidial germination and heat shock stress (36). Conidia play a key role in the virulence of pathogenic fungi, for example, in destructive hemibiotrophic phytopathogen *M. oryzae*, when its conidia are attached to the host surface, they can form appressorium, causing rice blast disease (37). However, the role of most sporulation-related genes is still unknown in NT fungi.

In this study, we investigated the homologous proteins MedA (AoMedA), BrlA (AoBrlA), AbaA (AoAbaA), and WetA (AoWetA) in *A. oligospora* via phenotypic comparison and multi-omics approaches. Our results showed that *AomedA* and three central regulatory genes (*AobrlA*, *AoabaA*, and *AowetA*) are required for conidiation, and they play divergent roles in trap formation, lipid droplet (LD) accumulation, autophagy, peroxisome, vacuole assembly, and secondary metabolism. We also detected the interaction between *AomedA* and three central regulatory genes using a yeast one-hybrid (Y1H) assay. In addition, the role and potential regulation of these sporulation-related genes were investigated by transcriptomic and metabonomic analyses.

RESULTS

Bioinformatic analysis of AoMedA, AoBrlA, AoAbaA, and AoWetA

Orthologs of MedA, BrlA, AbaA, and WetA were retrieved from *A. oligospora* based on the homologous sequences of *A. nidulans*. The partial sequence properties of these proteins are summarized in Table 1. The orthologs of MedA, BrlA, AbaA, and WetA were divided into different evolutionary branches (Fig. S1A), and they were highly homologous to orthologs derived from other NT fungi; for example, AoBrlA shared a high degree of sequence similarity with NT fungi *Arthrobotrys flagrans* (91.9%), *Drechslerella brochopaga* (60.7%), and *Dactylellina haptotyla* (77%), and it had a middle degree of similarity with *A. nidulans* (58.2%) (Fig. S1B).

AoMedA, AoBrlA, AoAbaA, and AoWetA are required for conidiation

Three mutants of each gene (*AomedA*, *AobrlA*, *AoabaA*, and *AowetA*) were generated, as described in the Materials and methods, and were then verified using PCR and Southern blot analyses (Fig. S2) using paired primers (Table 2). As independent mutant strains of each gene showed similar phenotypic traits, a single mutant from each gene was randomly selected for subsequent study. Deletion of *AomedA* resulted in a reduction in conidiophores and conidia yield when being compared with those in the wild-type (WT) strain (Fig. 1A and B). Moreover, the Δ*AobrlA* and Δ*AoabaA* mutants completely lost the ability to produce conidia and the Δ*AobrlA* mutant did not form conidiophores, whereas Δ*AoabaA* mutant could form conidiophores but not conidia (Fig. 1A and B). In particular, the Δ*AowetA* mutant produced deformed conidia (Fig. 1A), and the number of conidia by Δ*AowetA* mutant decreased compared with WT strain (Fig. 1B). Next, the stress response of conidia of WT and Δ*AowetA* mutant strains was tested with Congo red and menadione, and it was observed that the relative growth inhibition rate (RGI) of the Δ*AowetA* mutant increased remarkably under 0.05–0.07 mM menadione and 0.03–0.09 mg/mL Congo red compared with WT strain (Fig. 1C). Similarly, when the conidia of Δ*AowetA* mutant was treated at 42°C for 30 min, the germination ability of conidia was inhibited remarkably and approximately 89% and 36% of conidia had germinated in the WT and Δ*AowetA*, respectively. Moreover, the conidia of Δ*AowetA* mutant lost the ability to germinate when treated at 42°C for 1 h, whereas 70% conidia of WT strain could germinate (Fig. 1D). The trehalose content increased in Δ*AowetA* mutant from 3 to 7 d, whereas it decreased considerably from 9 to 11 d compared with the WT strain (Fig. 1E). In addition, conidia of WT and Δ*AowetA* mutant strains were observed by scanning electron microscopy (SEM), and it was observed that the conidia of Δ*AowetA* mutant attached on conidiophore had shrunk and the conidia of Δ*AowetA* mutant were abnormal (Fig. 1F). Furthermore, a high number of vacuoles and peroxisome-like structures were observed in the conidia of the Δ*AowetA* mutant by transmission electron microscopy (TEM) (Fig. 1G).

AoWetA had complex interactions with AoMedA, AoBrlA, and AoAbaA

The transcriptional level of sporulation-related genes in WT and mutant strains was determined by real-time quantitative PCR (RT-qPCR) analysis. Deletion of *AomedA* led to considerably increased transcription levels of *AovosA*, *AolreA*, *AoveA*, *AoflbA*, *AonsdD*, and

TABLE 1 Partial sequence properties of AoMedA and three central developmental regulators in *A. oligospora*

Gene	Open reading frame (bp)	Introns	Amino acid residues	Isoelectric point	Molecular weight (kDa)
AomedA	2018	2	608	9.16	67.14
AobrlA	966	0	321	7.34	35.39
AoabaA	1921	2	588	5.50	67.49
AowetA	2415	0	804	5.93	86.80

TABLE 2 Primers used for genetic manipulation

Primers	Sequence (5′–3′)	Description
AomedA_ZF	GTAACGCCAGGGTTTTCCCAGTCACGACGGATACCCACTTGACGACCCA	Amplify the *AomedA* gene 5′ flank
AomedA_ZR	ATCCACTTAACGTTACTGAAATCTCCAACGTAAGACCGGCTTCAGCGT	
AobrlA_ZF	GTAACGCCAGGGTTTTCCCAGTCACGACGGAAGGATGTGCGTGGCTCTA	Amplify the *AobrlA* gene 5′ flank
AobrlA_ZR	ATCCACTTAACGTTACTGAAATCTCCAACGGAGCTGGCATTTGTTTCCG	
AoabaA_ZF	GTAACGCCAGGGTTTTCCCAGTCACGACGCAACACTGCAAGGCTTCGTA	Amplify the *AoabaA* gene 5′ flank
AoabaA_ZR	ATCCACTTAACGTTACTGAAATCTCCAACAAGCTTCCTCAACCTCGTCA	
AowetA_ZF	GTAACGCCAGGGTTTTCCCAGTCACGACGCACTTCTTCACCCATCGGCT	Amplify the *AowetA* gene 5′ flank
AowetA_ZR	ATCCACTTAACGTTACTGAAATCTCCAACGATTCCGCGGAGACAGAGAG	
AomedA_YF	CTCCTTCAATATCATCTTCTGTCTCCGACTCGCGGTGTACTGTTTTCCA	Amplify the *AomedA* gene 3′ flank
AomedA_YR	GCGGATAACAATTTCACACAGGAAACAGCCGAGCCTCAGATCAGACGAAA	
AobrlA_YF	CTCCTTCAATATCATCTTCTGTCTCCGACTTATGGGTACGGGGGTCTGG	Amplify the *AobrlA* gene 3′ flank
AobrlA_YR	GCGGATAACAATTTCACACAGGAAACAGCGAGTTTGCGCTGCCAATTCA	
AoabaA_YF	CTCCTTCAATATCATCTTCTGTCTCCGACCCAGTCACATCCAGGTGTTG	Amplify the *AoabaA* gene 3′ flank
AoabaA_YR	GCGGATAACAATTTCACACAGGAAACAGCCCGTATCGACATTTGTGGTG	
AowetA_YF	CTCCTTCAATATCATCTTCTGTCTCCGACCGACGTTGAGGGGTTTGGAT	Amplify the *AowetA* gene 3′ flank
AowetA_YR	GCGGATAACAATTTCACACAGGAAACAGCAAAATCCCGCCTTTCACCGA	
Hph_F	GTCGGAGACAGAAGATGATATTGAAGGAGC	Amplify the *hph* cassette
Hph_R	GTTGGAGATTTCAGTAACGTTAAGTGGAT	
AomedA_F	TCCTCCACCATTCGATTATCAG	Verify the transformants
AomedA_R	GACAAGTGGCAAGATAGGTA	
AobrlA_F	CGGAAACAAATGCCAGCTCC	Verify the transformants
AobrlA_R	CCAGACCCCCGTACCCATAA	
AoabaA_F	CAACACTGCAAGGCTTCGTA	Verify the transformants
AoabaA_R	CCGTATCGACATTTGTGGTG	
AowetA_F	CTCTCTGTCTCCGCGGAATC	Verify the transformants
AowetA_R	ATCCAAACCCCTCAACGTCG	
AomedA_TZF	GTTTGAAGACCGTTCCACCA	Make Southern blotting probe
AomedA_TZR	TGCTCAGACTCAGATGGACG	
AobrlA_TZF	AGCCTGCCCAGTAATATGTATCG	Make Southern blotting probe
AobrlA_TZR	GCTGGCATTTGTTTCCGAAGA	
AoabaA_TZF	TCTAAGACACGGGCTGCAAG	Make Southern blotting probe
AoabaA_TZR	GGTGGTGTTTGTAAAGGTCGC	
AowetA_TZF	TTTGCCTCGAGTCGGTTCTC	Make Southern blotting probe
AowetA_TZR	TGCTAAAACCGCGTTCAAAGG	

AowetA, whereas *AoabaA*, *AofluG*, *AobrlA*, and *Aohyp1* were considerably downregulated (Fig. 2A). In Δ*AobrlA* mutant, the transcripts of *AolreA*, *AowetA*, *AoflbA*, and *AomedA* were upregulated, whereas *AofluG*, *AoabaA*, and *Aohyp1* were downregulated (Fig. 2B). In Δ*AoabaA* mutant, only the *AowetA* gene was upregulated but *AofluG* and *Aohyp1* were downregulated (Fig. 2C). In Δ*AowetA* mutant, *AomedA*, *Aohyp1*, and *AobrlA* were considerably upregulated, whereas *AolreB* was considerably downregulated (Fig. 2D). Y1H assay showed that AoBrlA can physically bind to the promoter region of AoMedA, AoAbaA, and AoWetA; meanwhile, both AoMedA and AoAbaA can bind to AoWetA (Fig. 2E).

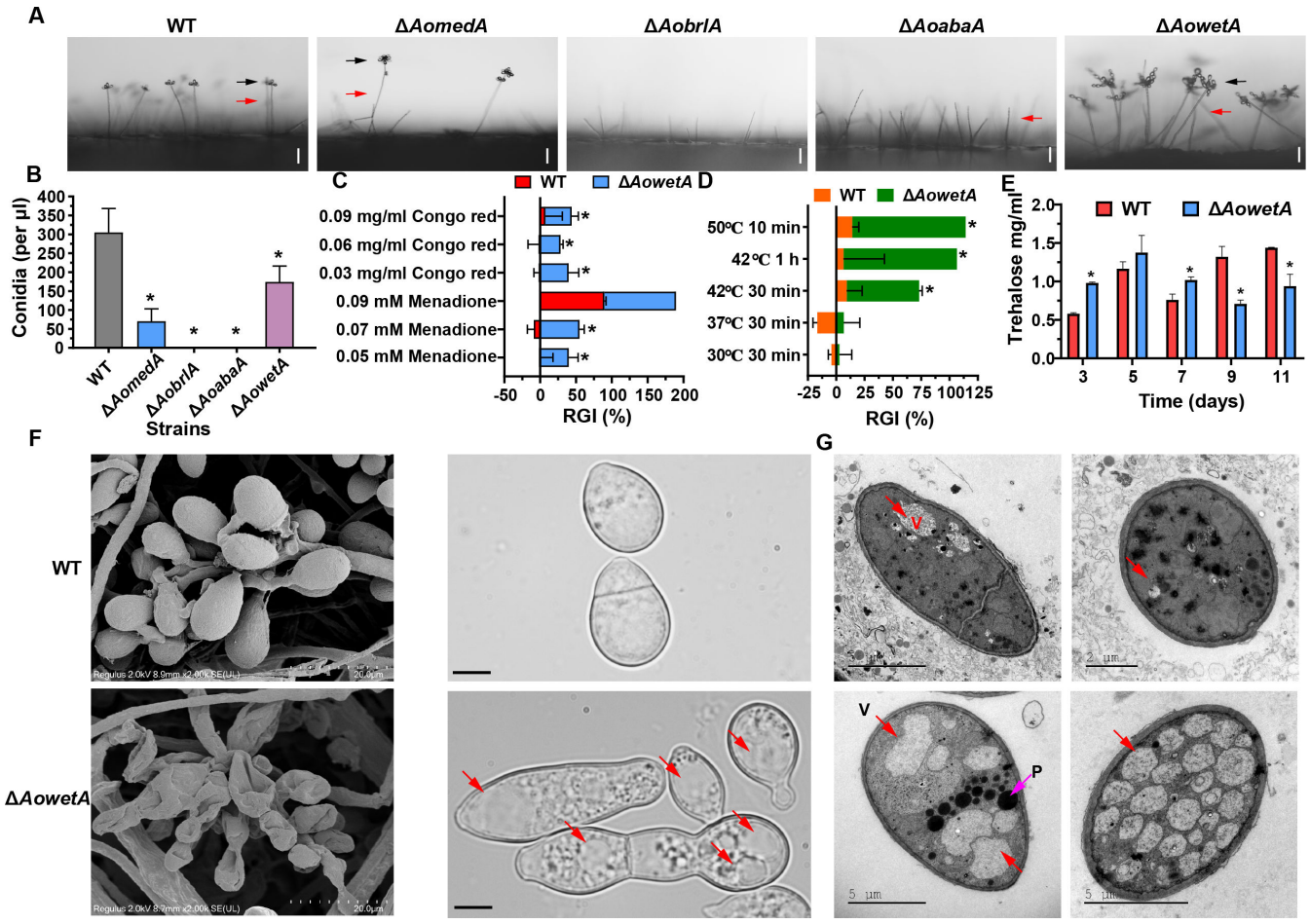

FIG 1 Comparison of conidiophores and conidia between WT and mutant strains. (A) Conidiophores and conidia of WT and mutant strains were observed under a light microscope. Bar = 10 µm. Red arrows indicate conidiophores, and black arrows indicate conidia. (B) Comparison of conidia yields. (C) Stress tolerance of conidia of WT and Δ*AowetA* mutant strains to chemical reagents. (D) Stress tolerance of conidia of WT and Δ*AowetA* mutant strains to heat shock. (E) Comparison of trehalose content. (F) Observation of conidiophores and conidia of WT and Δ*AowetA* mutant strains using a scanning electron microscope (SEM). Red arrows indicated vacuole. (G) Observation of ultrastructure of conidia of WT and Δ*AowetA* mutant strains under a transmission electron microscope. Red arrows indicate vacuoles and pink arrow indicates peroxisome-like structures. Asterisk (B–E) indicates a significant difference between mutant and WT strain (Tukey's HSD, $P < 0.05$).

AoMedA and three regulators play divergent roles in trap formation and pathogenicity

The Δ*AomedA* mutant lost the ability to form traps, and nematode mortality reduced remarkably (Fig. 3A), but the mycelium of the Δ*AomedA* mutant could still penetrate and decompose nematodes. Furthermore, many LDs were observed in the mycelia of Δ*AomedA* mutant after induction with nematodes, whereas electron-dense bodies (EDs) disappeared (Fig. 3B). The deletion of *AobrlA*, *AoabaA*, and *AowetA* genes resulted in increased trap formation than WT strain, and at 12 h post-induction (hpi), the average number of traps formed by Δ*AobrlA* and Δ*AoabaA* strains was 1021 and 627, respectively, which was higher than that of WT strain (179 traps), and the nematode mortality (53.36%) of Δ*AoabaA* strains increased considerably, whereas that of WT strain was 16.13%. At 24, 36, and 48 hpi, the number of traps formed by Δ*AobrlA*, Δ*AoabaA*, and Δ*AowetA* strains was also considerably more than that of the WT strain, whereas nematode mortality was not different from WT strain, except for the Δ*AowetA* mutant, which showed remarkable reduction in nematode mortality at 24 hpi (Fig. 3C and D). Furthermore, the ultrastructures of trap cells were observed by TEM, and the traps of WT, Δ*AobrlA*, Δ*AoabaA*, and Δ*AowetA* mutants were filled with EDs and separation of the

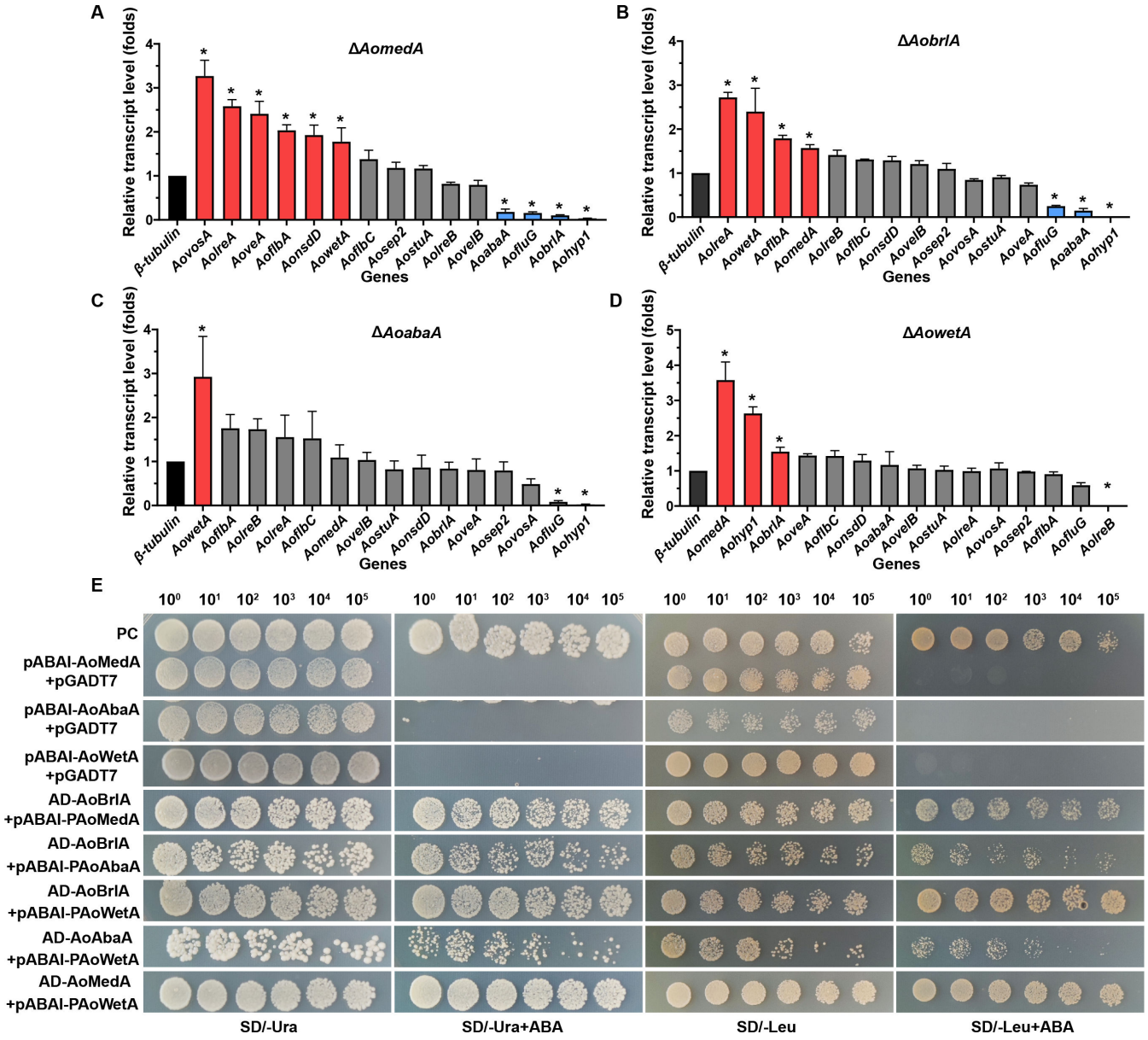

FIG 2 Comparison of relative transcription levels (RTLs) of sporulation-related genes between WT and mutant strains and yeast one-hybrid assay. (A–D) Comparison of RTLs of sporulation-related genes in Δ*AomedA* (A), *AobrlA* (B), *AoabaA* (C), and Δ*AowetA* mutants (D) versus WT strain. Error bars: SD from three replicates. Asterisk (A–D) indicates a significant difference between mutant and WT strain (Tukey's HSD, $P < 0.05$). (E) Yeast one-hybrid assay of AoMedA, AoBrlA, AoAbaA, and AoWetA. pGADT7-Rec-p53/p53-AbAi as positive control and pABAI-AoMedA, pABAI-AoAbaA, and pABAI-AoWetA plus pGADT7 as negative controls. Yeast transformants were diluted in 0.9% NaCl, and serially diluted five times with equal volume for obtaining 10^0, 10^{-1}, 10^{-2}, 10^{-3}, 10^{-4}, and 10^{-5} dilutions.

plasma membrane and cell wall occurred in the trap cells of the three mutant strains (Fig. 3B).

AoMedA and three regulators play pleiotropic roles in mycelial growth, hyphal septum, cell nucleus, and LD accumulation

The colony and mycelial morphology of WT and mutant strains were observed in tryptone–yeast extract–glucose (TYGA) medium. Compared with the WT strain, the aerial hyphae of the Δ*AomedA* mutant were sparse, whereas the colony grew intensively; the aerial hyphae of Δ*AobrlA* mutant were extremely thriving, but the aerial hyphae of

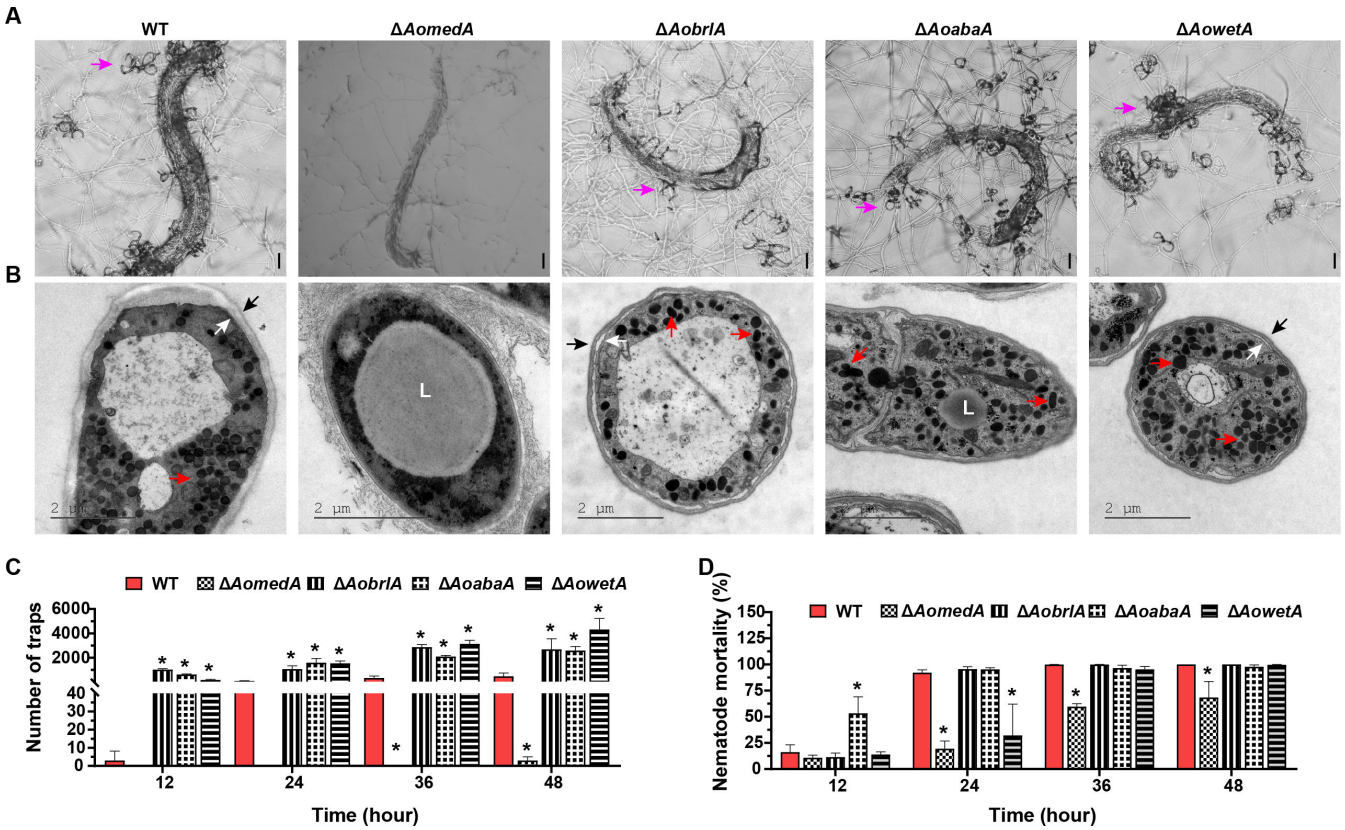

FIG 3 Comparison of trap formation and pathogenicity between WT and mutant strains. (A) Observation of trap formation and captured nematodes using a light microscope. Bar = 50 μm. Pink arrows indicate traps. (B) Observation of ultrastructure of traps using TEM. Blank arrows indicate cell wall, white arrows indicate cell membrane, red arrows indicate electron-dense bodies, and L indicates lipid droplets. (C) Comparison of the number of traps. (D) Comparison of nematode mortality. Error bars: SD from three replicates. Asterisk (C and D) indicates a significant difference between mutant and WT strain (Tukey's HSD, $P < 0.05$).

Δ*AoabaA* mutant became very compact, whereas the growth of aerial hyphae of Δ*AowetA* mutant was comparable with WT strain (Fig. 4A). Moreover, the radial growth of Δ*AomedA* mutant was remarkably slower on potato dextrose gar (PDA) or tryptone–glucose (TG) media, and the growth of Δ*AobrlA*, Δ*AoabaA*, and Δ*AowetA* mutants was mired on TG medium, whereas the growth was consistent with WT strain on PDA medium (Fig. 4B). The hyphal septum was observed using calcofluor white (CFW) dye (Fig. 4C), more septa were observed in Δ*AomedA* mutant, and the average length of mycelial cells of Δ*AomedA* mutant was considerably shorter, whereas the mycelial length of Δ*AobrlA* and Δ*AoabaA* was considerably longer than that of WT strain (Fig. S3A). In addition, mycelial nuclei were visualized by staining with 4′,6-diamino-2-phenylindole (DAPI) (Fig. 4D), the number of nuclei in WT strain was 7.0 per cell, and the number of nuclei in Δ*AomedA*, Δ*AobrlA*, Δ*AoabaA*, and Δ*AowetA* mutants was 5.0, 4.0, 4.0, and 6.0, respectively (Fig. S3B). When mycelial samples were stained with boron–dipyrromethene (BODIPY) (Fig. 5A), the fluorescence intensity of LDs in Δ*AobrlA* mutant was less than that of WT and the other three mutant strains. In addition, the volume of LDs in Δ*AomedA* mutant was higher than that of WT, and the number of LDs in Δ*AoabaA*, Δ*AobrlA*, and Δ*AowetA* was less than the WT strain (Fig. S3C). In addition, the mycelia of Δ*AomedA* and Δ*AoabaA* mutants formed trap-like structures when they were incubated on water agar (WA) plates (Fig. 5B and C).

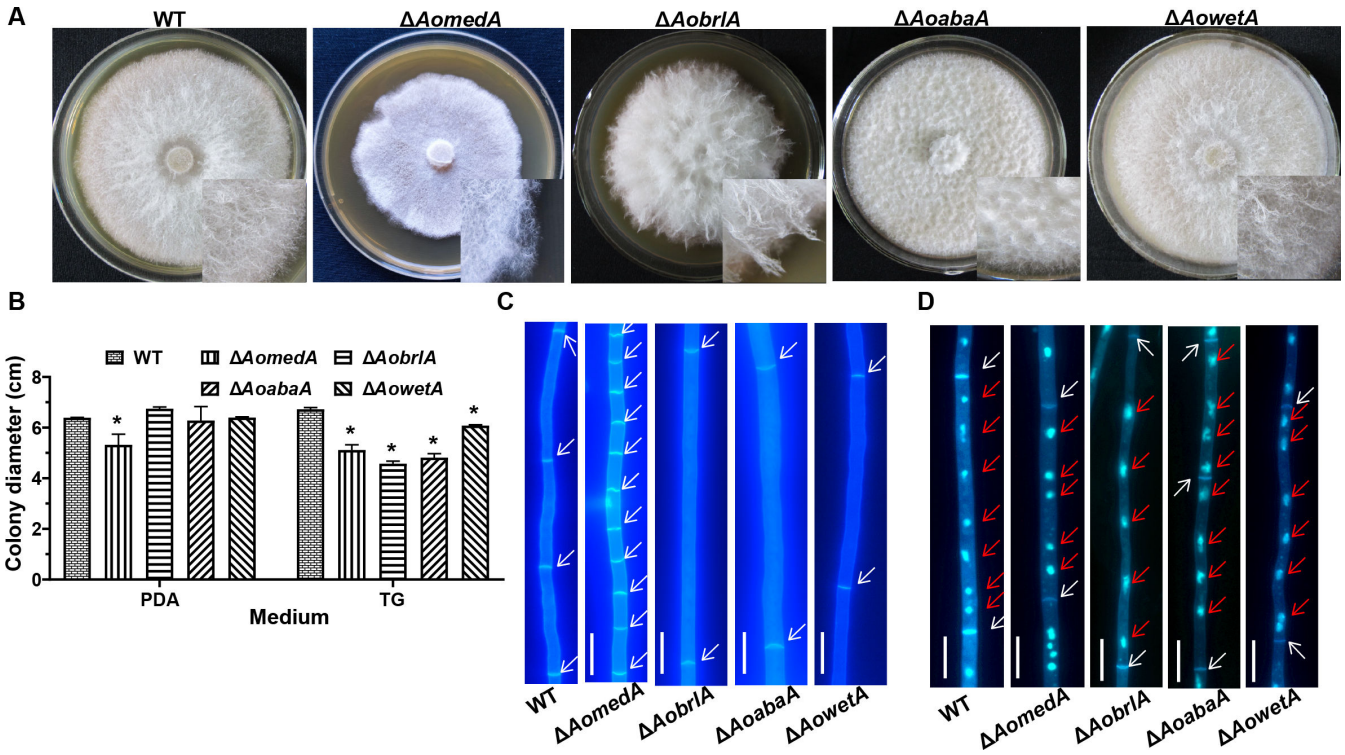

FIG 4 Comparison of mycelial growth, septa, and nuclei between WT and mutant strains. (A) Colony morphology of WT and mutant strains incubated on TYGA medium for 5 d. (B) Comparison of colony diameters of WT and mutant strains incubated on PDA and TG medium for 5 d. Error bars: SD from three replicates. Asterisk indicates a significant difference between mutant and WT strain (Tukey's HSD, $P < 0.05$). (C) Mycelial cells were stained with CFW dye. White arrows indicate cell septa of the hyphae. (D) The nuclei of mycelial cells were stained using CFW and DAPI. White arrows indicate the cell septa of hyphae, and red arrows indicate nuclei. Bar = 10 µm.

AoMedA and three regulators play crucial roles in vacuole assembly

The vacuoles in the mycelia of WT and mutant strains were observed by 7-amino-4-chloromethylcoumarin (CMAC) staining, and the vacuoles in the WT strain were usually regular round and long oval, whereas the vacuoles were small and fragmented in the hyphal cells of Δ*AomedA* mutant and were irregular, elongated, and almost occupied the whole mycelial cell in Δ*AobrlA* mutant, and the vacuoles in Δ*AoabaA* strains mostly existed in the form of long ellipses. Although there was no difference in vacuole morphology between WT and Δ*AowetA* mutant strains, several pexophagy-like structures were observed in most vacuoles of Δ*AowetA* mutant (Fig. 6A). Furthermore, similar results of vacuoles were observed in the mycelia of WT and mutants by TEM (Fig. 6B).

AoMedA and AoWetA participate in the regulation of autophagy and peroxisome

Mycelial samples of WT, Δ*AomedA*, and Δ*AowetA* strains were stained with monodansylcadaverine (MDC), and the Δ*AomedA* and Δ*AowetA* mutants had higher fluorescence intensities than that of the WT strain (Fig. 7A through C; Fig. S3D). Furthermore, more autophagosome-like structures were observed in the two mutants than WT strain (Fig. 7A through C). The mycelia of WT, Δ*AomedA*, and Δ*AowetA* mutant strains were collected and lysed to obtain proteins for Western blot analysis with p62 antibody (autophagosome marker). The results showed that autophagy in Δ*AomedA* and Δ*AowetA* mutants was considerably higher than that in the WT strain (Fig. 7D). In addition, the results of Western blot analysis with Pex5 and Pex7 antibody (peroxisome marker) showed that Pex5 in Δ*AomedA* and Pex7 in Δ*AowetA* mutants were considerably higher than that in WT strain, respectively (Fig. 7E).

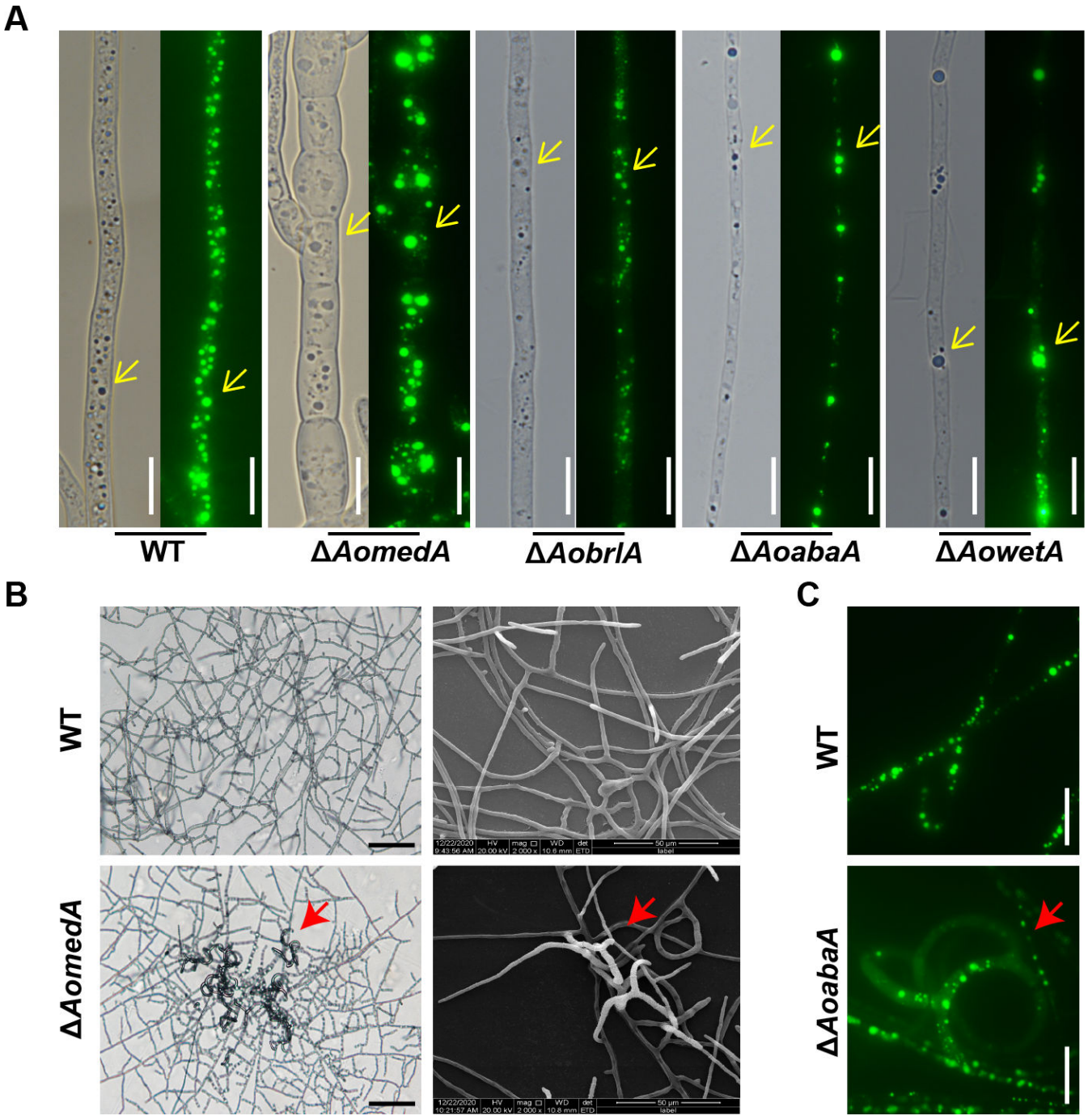

FIG 5 Comparison of the lipid droplets between WT and mutant strains. (A) Lipid droplets were stained by BIODIPY and observed using a light microscope (left panel) and fluorescence electron microscope (right panel), respectively. Yellow arrows indicate lipid droplets. (B) Observation of mycelial morphology of WT and Δ*AomedA* mutant strains by light microscopy (left panel) and SEM (right panel). The red arrow indicates the trap-like structure produced by Δ*AomedA* mutant. (C) Observation of mycelial morphology of WT and Δ*AoabaA* mutant strains by fluorescence electron microscopy. The red arrow indicates the trap-like structure produced by Δ*AomedA* (B) and Δ*AoabaA* (C) mutants. Bar (A and C) =10 µm.

Analysis of transcriptome profiles of the WT, Δ*AomedA*, and Δ*AowetA* mutant strains

To further explore the regulation mechanism of conidiation in *A. oligospora*, mixed samples of hyphae and conidia of WT and mutant (Δ*AomedA* and Δ*AowetA*) strains were collected for transcriptome analysis, and sequencing statistics showed that the genes in

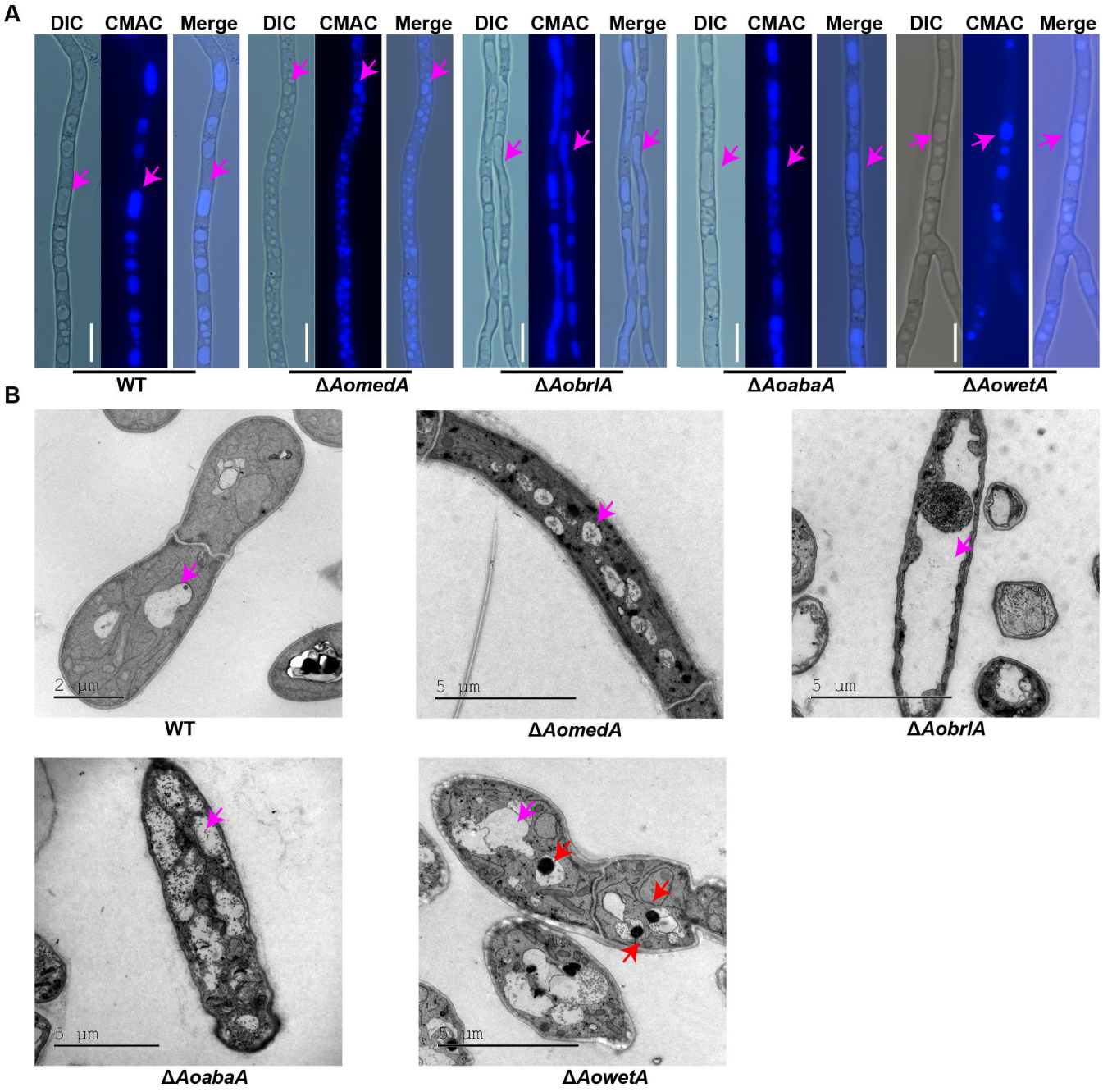

FIG 6 Comparison of vacuole morphology and ultrastructure of hyphae between WT and mutant strains. (A) Observation of vacuole morphology stained using 7-amino-4-chloromethylcoumarin (CMAC). Pink arrows indicate vacuoles. Bar = 10 μm. (B) Observation of ultrastructure of WT and mutant strains by TEM. Pink arrows indicate vacuoles, and red arrows indicate pexophagy-like structures.

each group were expressed efficiently (Table S1). Principal components analysis (PCA) showed that the three repeats of each sample shared a high degree of similarity (Fig. S4A). The accuracy of the transcriptomic data were confirmed by RT-qPCR of genes associated with endocytosis, phagosome, lipid metabolism, cell growth, and peroxisome (Fig. S4B and C).

There were 1,844 upregulated differentially expressed genes (DEGs) and 1,334 downregulated DEGs in Δ*AomedA* mutant versus WT strain, there were 1,536 upregulated DEGs and 837 downregulated DEGs in Δ*AowetA* mutant versus WT strain, and 1,430 DEGs were shared in the Δ*AomedA* and Δ*AowetA* mutants, of which 1,039 were

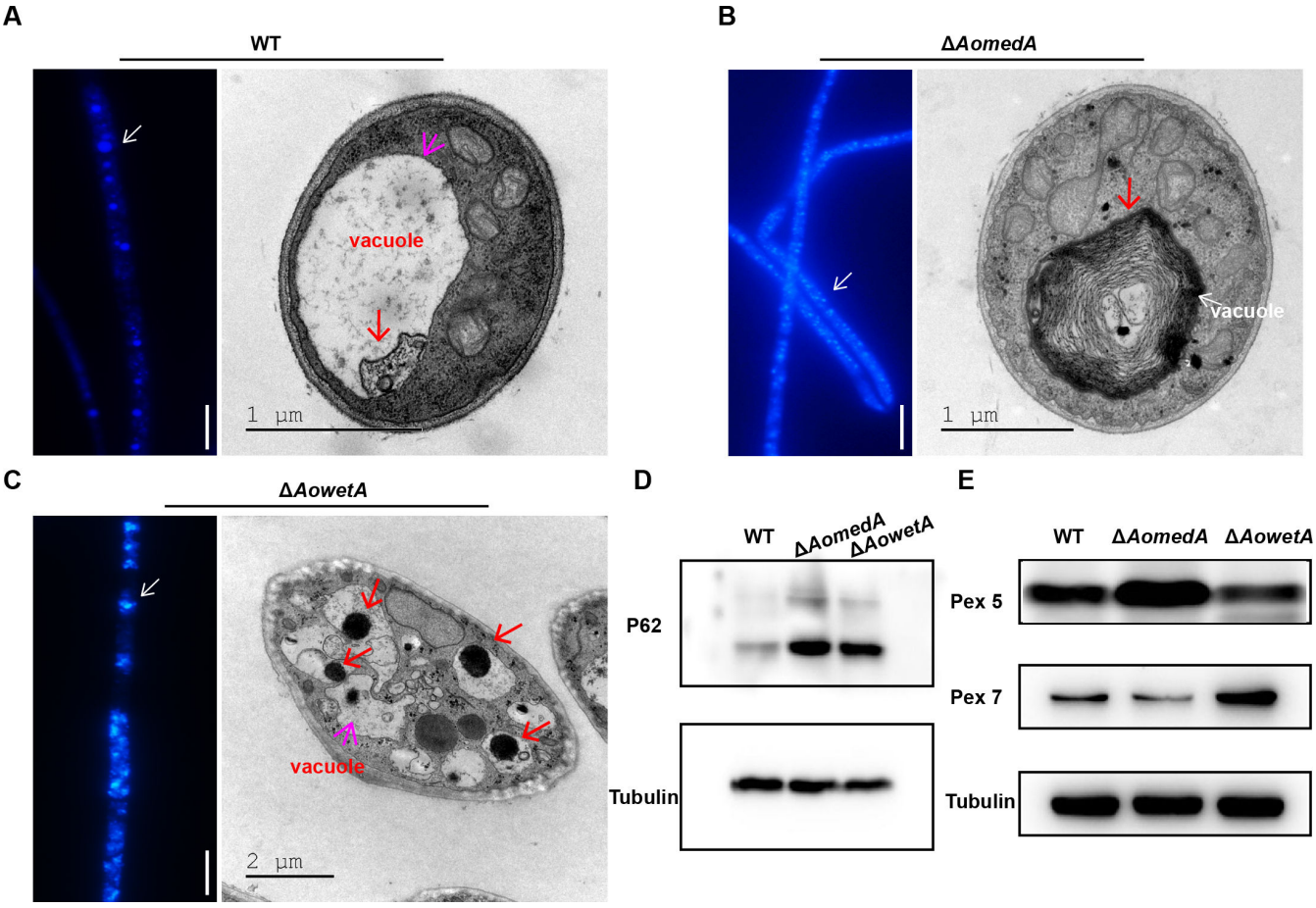

FIG 7 Detection of autophagy in WT and mutants (Δ*AomedA* and Δ*AowetA*). (A–C). Observation of autophagic vesicles of WT strain (A), Δ*AomedA* (B), and Δ*AowetA* (C) mutants stained by MDC (left panel) and observed by TEM (right panel). (D) Western blot analysis of autophagy in WT and mutant strains. Anti-SQSTM1/p62 antibody was used as an autophagosome marker and tubulin as the control. (E) Western blot analysis of peroxisome in WT and mutant strains. Anti-PEX5/PER3 antibody and anti-PEX7 antibody were used as peroxisome markers and tubulin as the control.

upregulated and 354 genes were downregulated in both groups (Fig. 8A). There were 17 sporulation-related DEGs in both groups. In gene co-expression analysis, deletion of *AomedA* and *AowetA* revealed that *AobrlA* played a central role in conidiation, which connected with *AosfgA* and *AoabaA*. *AosfgA* was linked with *AowetA*, *AowetA* was linked with *AopkaA*, and *AopkaA* was linked with *AomedA*; these genes were linked with other genes and constituted a complex network to regulate conidiation (Fig. 8B).

Gene Ontology (GO) and Kyoto encyclopedia of genes and genomes (KEGG) enrichment analyses were performed for these 1,430 DEGs, and GO enrichment analysis showed that intrinsic component of membrane and integral component of membrane were considerably enriched in cellular component; chromosome condensation, mitotic chromosome condensation, cellular carbohydrate biosynthetic process, and lipid catabolic process were considerably enriched in biological process; and two categories UDP-glucosyltransferase activity and D-alanine-D-alanine ligase activity were enriched in molecular function (Fig. 8C). Unlike these, upregulated DEGs in Δ*AomedA* mutant versus WT strain were also considerably enriched in transmembrane transport, transport, establishment of localization, localization, and obsolete oxidation–reduction process, whereas downregulated DEGs were enriched in organic acid metabolic process, cellular amino acid metabolic process, small molecule biosynthetic process, and organic acid biosynthetic process (Fig. S5). The upregulated DEGs of Δ*AowetA* mutant versus WT strain were also considerably enriched in transmembrane transport and membrane, whereas

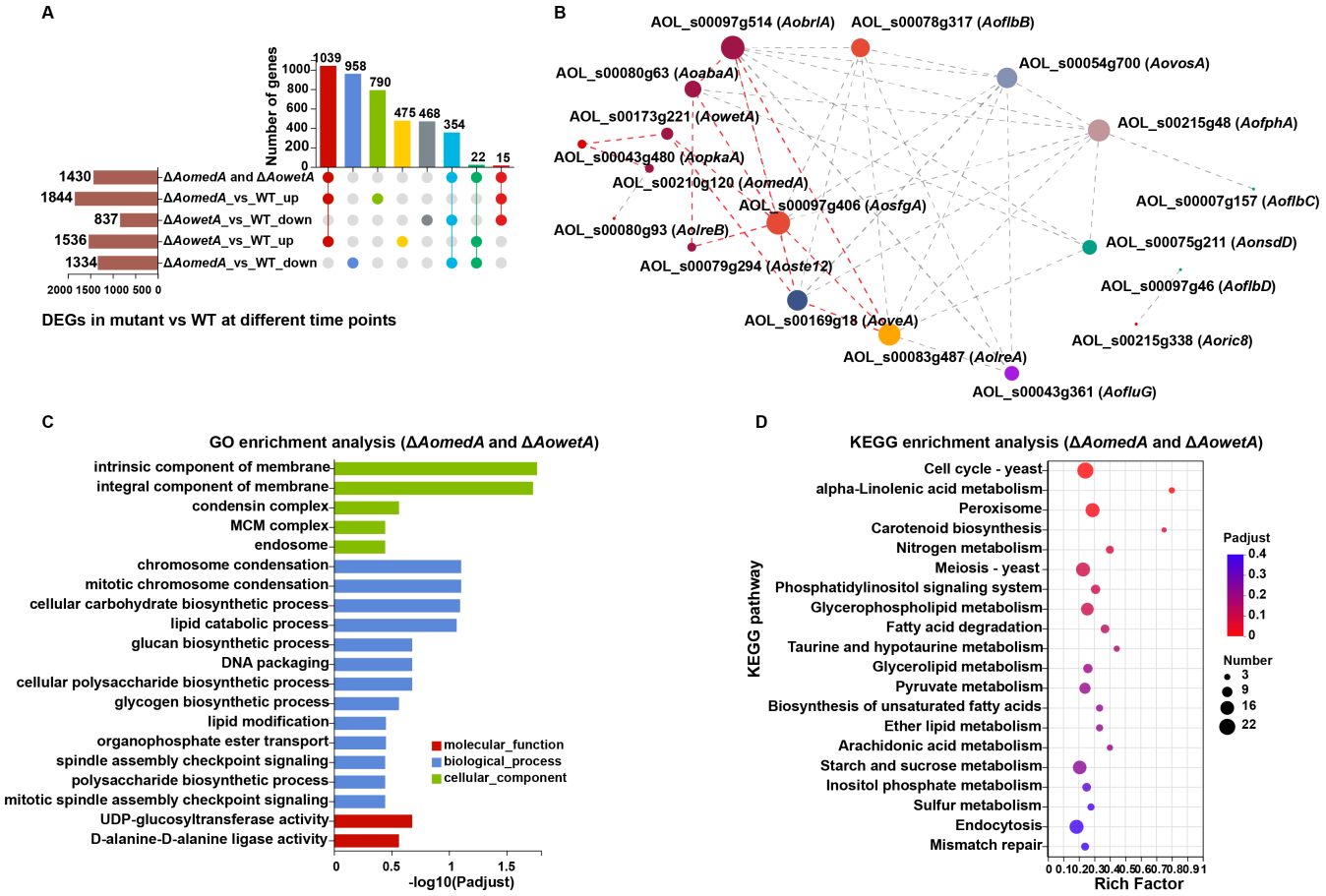

FIG 8 Comparison of DEGs in WT and mutants (Δ*AomedA* and Δ*AowetA*). (A) UpSet plot analysis of DEGs between Δ*AomedA*/Δ*AowetA* mutant versus WT strain. The bar chart on the bottom left represents the number of the up/downregulated DEGs. The dotted line at the bottom right shows the number of DEGs in the different groups. (B) Visual representation of gene expression correlation of sporulation-related genes. In the figure, each node represents a gene/transcript and the connection between nodes represents the correlation between gene/transcript expression. The size of nodes indicates the transcript levels of genes/transcripts, and indicates the transcript correlation between different genes/transcripts. Node size is positively correlated with transcription level of gene/transcript. (C) Gene Ontology (GO) enrichment analysis of DEGs of Δ*AomedA* and Δ*AowetA* mutants versus WT strain. (D) Kyoto encyclopedia of genes and genomes (KEGG) pathway analysis of Δ*AomedA* and Δ*AowetA* mutants versus WT strain.

downregulated DEGs were enriched in catalytic activity, organic substance metabolic process, cellular process, and nitrogen compound metabolic process (Fig. S6).

KEGG enrichment analysis showed that genes of cell cycle, peroxisome, meiosis, glycerophospholipid metabolism, pyruvate metabolism, starch and sucrose metabolism, and endocytosis were enriched (Fig. 8D). Upregulated DEGs of Δ*AomedA* mutant versus WT strain were considerably enriched in linoleic acid metabolism, longevity regulating pathway, phagosome, cyanoamino acid metabolism, and fructose and mannose metabolism, and downregulated DEGs were enriched in DNA replication; homologous recombination; aminoacyl-tRNA biosynthesis; lysine biosynthesis; cysteine and methionine metabolism; nucleotide excision repair; valine, leucine, and isoleucine biosynthesis; glycine, serine, and threonine metabolism; and protein processing in the endoplasmic reticulum (Fig. S5). The interaction network analysis of AoMedA protein showed that AoMedA can regulate endocytosis, phagosome, lipid metabolism, cell growth, and peroxisome (Fig. S7A). Yeast two-hybrid (Y2H) assay showed that AoMedA can interact with AOL_s00054g434 (Fig. S7B), which encodes the transcription factor Atf21. Upregulated DEGs of Δ*AowetA* mutant versus WT strain were considerably enriched in ABC transporters and valine, leucine, and isoleucine degradation, whereas ribosome biogenesis in eukaryotes, aminoacyl-tRNA biosynthesis, ubiquinone and other

terpenoid–quinone biosynthesis, DNA replication, and glycosaminoglycan degradation were enriched in downregulated DEGs (Fig. S6).

AoMedA and three regulators play a different role in secondary metabolism

Crude extracts of WT and mutant strains were detected by ultra-performance liquid chromatography (UPLC)–mass spectrometry (MS), and the chromatogram analysis showed that the peak values and secondary metabolites of Δ*AomedA* and Δ*AoabaA* mutants decreased considerably compared with the WT strain. The peak value of Δ*AobrlA* mutant decreased considerably to 12 min from 23–38 min, whereas the peak value of Δ*AowetA* mutant exhibited no difference from WT strain (Fig. 9A). Volcanic map analyses showed that more downregulated compounds were detected in the mutants Δ*AomedA*, Δ*AoabaA*, and Δ*AobrlA* compared with WT strain (Fig. S8A through D). KEGG pathway analysis showed that metabolic pathways, biosynthesis of secondary metabolites, microbial metabolism in diverse environments, degradation of aromatic compounds, and biosynthesis of cofactors were considerably enriched in the three mutant strains Δ*AomedA*, Δ*AoabaA*, and Δ*AobrlA*. In addition, alpha-linolenic acid metabolism and bisphenol degradation were particularly enriched in Δ*AomedA* mutant; 2-oxocarboxylic acid metabolism was enriched in Δ*AobrlA*, Δ*AoabaA*, *and* Δ*AowetA* mutants; and steroid hormone biosynthesis was enriched in Δ*AobrlA* and Δ*AoabaA* mutants (Fig. 9B).

The peak of arthrobotrisins was analyzed in WT and mutant strains, which was detected at 35 min, and the mass spectra were 139, 393, and 429 m/z (Fig. S8E). The content of arthrobotrisins in Δ*AobrlA* and Δ*AoabaA* mutants was less than that of WT strain, and no arthrobotrisins were detected in Δ*AomedA* mutant (Fig. 9C). Transcriptional level of the 215 g gene cluster associated with the biosynthesis of arthrobotrisins was analyzed, and most of these genes were downregulated in Δ*AomedA* and Δ*AowetA* mutants versus WT strain (Fig. 9D).

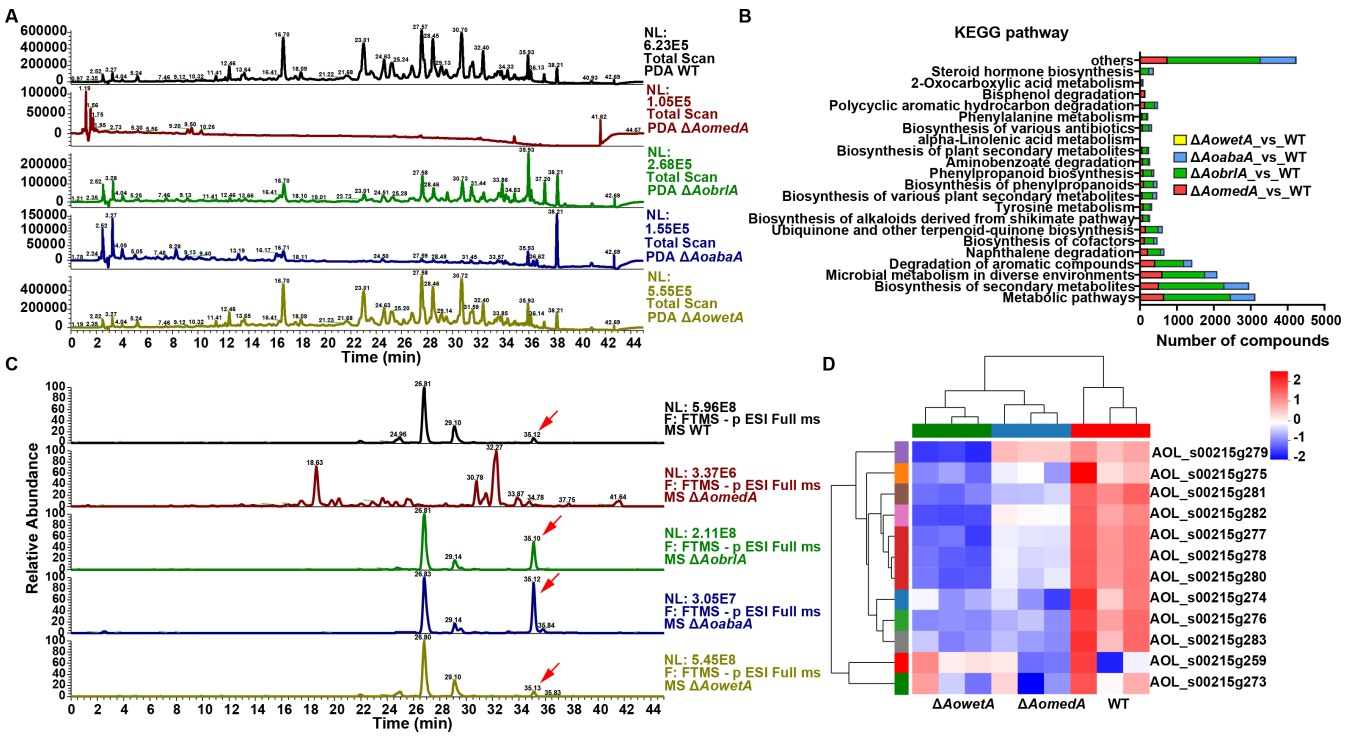

FIG 9 Comparison of secondary metabolism between WT and mutant strains. (A) Comparison of UPLC-MS profiles of WT and mutant strains. (B) Comparison of KEGG pathways of mutant versus WT strains. (C) Detection of the peak of arthrobotrisins in the chromatogram. The red arrow indicates the peak of arthrobotrisins. (D) Heatmap shows the relative transcript levels of genes associated with the biosynthesis of arthrobotrisins in WT, Δ*AomedA*, and Δ*AomedA* mutant strains.

DISCUSSION

Asexual sporulation (conidiation) is the most common reproductive mode for many filamentous fungi, and the number of genes involved in conidiation has been identified, particularly, a FluG-mediated conidiation signaling pathway has been proposed for several filamentous fungi (38). In this study, we characterized the developmental regulator AoMedA and three core regulatory proteins AoBrlA, AoAbaA, and AoWetA in *A. oligospora* as they are crucial for conidiation and trap formation and play pleiotropic roles in mycelial development, LD accumulation, autophagy, vacuole assembly, and secondary metabolism.

The crucial role of MedA and three core regulatory proteins in conidiation has been revealed in several filamentous fungi. Mutations in the developmental modifier MedA resulted in frequent reinitiation of secondary conidiophores in *A. nidulans* (39). Similarly, deletion of *AomedA* caused the formation of secondary conidiophores in *A. oligospora*, and the conidia yield of Δ*AomedA* mutant decreased remarkably compared with that in the WT strain, which is consistent with *A. fumigatus* (40), whereas Δ*AomedA* mutant produced more mature conidia with a septum, possibly associated with high expression of *AovosA* and *AowetA*, as VosA and WetA are indispensable for conidia maturation (11). Δ*AobrlA and* Δ*AoabaA* strains completely lost the ability to produce conidia, and the results were consistent with *A. nidulans* (41), *A. oryzae* (42), *B. bassiana* (16), and *Metarhizium robertsii* (43). Based on our results, *AobrlA* is essential for conidiophore development and *AoabaA* is required for the formation of conidia, but there was no effect on conidia in Δ*brlA* mutant of *Monascus ruber M7* (44) and Δ*brlA* mutant of *Neurospora crassa* (45). Δ*AowetA* mutant produced conidia, but the conidial yields decreased, which is similar to that observed in *M. robertsii* (18), and many conidia were immature with no septum, as observed in *Fusarium graminearum* (46). In particular, the morphology of the conidia of Δ*AowetA* mutant was acutely deformed and the cytoplasm of the conidia was filled with vacuoles. In addition, Δ*AowetA* strains were more sensitive to chemical stress reagents (Congo red and menadione) and high temperature, as also observed in *B. bassiana* (17) and *P. digitatum* (13). Moreover, the trehalose content in Δ*AowetA* strains changed with the culture times, which was different from *B. bassiana* (17), *Aspergillus flavus* (47), and *A. fumigatus* (11). Taken together, *AomedA*, *AobrlA*, *AoabaA*, and *AowetA* play a conserved and distinct role in conidiation in *A. oligospora* and other filamentous fungi.

At the transcriptional level, *AomedA*, *AobrlA*, and *AoabaA* had negative feedback regulation with *AowetA*. *AobrlA* had negative feedback regulation with *AomedA* but had positive regulation with *AoabaA*. Y1H assay revealed that AoBrlA regulated AoMedA, AoAbaA, and AoWetA and AoMedA and AoAbaA regulated AoWetA. The regulation relationship of AoBrlA, AoAbaA, and AoWetA was the same as in *M. robertsii* (18), whereas the regulation relationship between AoMedA and AoBrlA was different from MedA and BrlA in *Penicillum chrysogenum*; the deletion of *brlA* had no effect on *medA* (48), and the regulation relationship of AoBrlA, AoAbaA, and AoWetA was different from BrlA, AbaA, and WetA in *A. nidulans* (41) and *P. digitatum* (13) at the transcript level. The inactivation of *brlA* inhibits the expression of *abaA* and *wetA*, whereas the inactivation of *abaA* inhibits the expression of *wetA*. Therefore, the regulation relationships of *AomedA*, *AobrlA*, *AoabaA*, and *AowetA* were varied in fungal species, which implied that asexual sporulation is very complex in filamentous fungi and could be affected by various factors.

Conidiation is usually closely related to the pathogenicity of fungi (49). In this study, *AomedA*, *AobrlA*, *AoabaA*, and *AowetA* as the core regulatory genes in conidiation also had important roles in trap formation and pathogenicity. In Δ*AomedA* mutant, trap formation was completely abolished; therefore, the pathogenicity of Δ*AomedA* mutant decreased remarkably compared with the WT strain, which is similar to studies on *A. fumigatus* (40), *Ustilago maydis* (50), and *M. grisea* (15, 51). Conversely, Δ*AobrlA*, Δ*AoabaA*, and Δ*AowetA* mutants produced more traps than the WT strain, the pathogenicity of Δ*AoabaA* mutant increased remarkably at 12 hpi, and the pathogenicity of Δ*AowetA* mutant decreased remarkably at 24 hpi, whereas their pathogenicity had no difference

from WT strain at 36 and 48 hpi. In *M. robertsii* (43) and *B. bassiana* (16), *brlA* and *abaA* strains had no conidia and reduced colonization capacity to host, and in *F. graminearum*, AbaA and WetA were indispensable for conidiation while not for virulence (46, 52). Thus, the orthologs of MedA, BrlA, AbaA, and WetA play a varied role in the pathogenicity of different fungal species and are crucial for trap formation in *A. oligospora*.

A previous study indicated that Δ*medA* mutant had deficient mycelial growth in *U. maydis* (50). In this study, the deletion of *AomedA* caused a reduction in mycelial growth and the number of nuclei but increased hyphal septa, LD accumulation, and autophagy, particularly, the deletion of *AomedA* impaired vacuole assembly. In contrast, Δ*AobrlA*, Δ*AoabaA*, and Δ*AowetA* mutants had no significant difference in PDA compared with the WT strain, but their growth was decelerated on TG medium, and the average length of mycelia cells of Δ*AobrlA* and Δ*AoabaA* strains increased. In contrast to our results, BrlA, AbaA, and WetA are essential for conidiation but not for mycelial growth in *B. bassiana* (16) and *F. graminearum* (46). In addition, the deletion of *AobrlA* and *AoabaA* resulted in a reduction in hyphal septa, number of nuclei, and LD accumulation, and the vacuole became bigger and was filled with hyphal cells. Similarly, the deletion of *AowetA* reduced the number of nuclei and LD accumulation. Moreover, Δ*AomedA* and Δ*AoabaA* mutants formed a trap-like structure, and Δ*AomedA* and Δ*AowetA* mutants had a high autophagic level compared with the WT strain. Therefore, AoMedA and three core regulatory proteins play an important role in mycelial growth, nuclei, LD accumulation, vacuole assembly, and autophagy, whereas their roles are varied in *A. oligospora*.

Transcriptome analysis is considered a robust method to study differential gene expression in organisms under different sets of conditions (53). Here, RNA-Seq was performed to analyze differential gene expression caused by the deletion of sporulation-related genes. We focused on common DEGs of Δ*AomedA* and Δ*AowetA* mutants compared with WT strain and observed that several pathways, such as lipid catabolic and modification process, cell cycle, peroxisome, nitrogen metabolism, meiosis, glycerophospholipid metabolism, pyruvate metabolism, and endocytosis, were enriched. Lipid catabolic and modification process may be associated with the altered LD accumulation in Δ*AomedA* and Δ*AowetA* strains. Similarly, peroxisomes are associated with EDs, which contain existing trap cells (54–56). In our previous studies, several peroxisome biogenesis genes were identified in *A. oligospora*, and they were indispensable for conidiation and trap formation (34, 35). Here, the deletion of *AomedA* caused the loss of trap formation. In addition, nitrogen metabolism and endocytosis may be associated with autophagy (56, 57), and the deletion of *AomedA* and *AowetA* genes facilitated autophagy. A combination of transcriptome analysis and Y2H verification revealed that AoMedA can interact with AOL_s00054g434 that encodes the transcription factor Atf21; Atf21 participates in meiosis, osmotic pressure reaction, and sporulation in fission yeast (58), but the function of Atf21 has not been revealed in filamentous fungi. Therefore, many enriched pathways in transcriptome coincide well with the phenotypic features of Δ*AomedA* and Δ*AowetA* mutants.

Secondary metabolites produced by NT fungi, which act as chemoattractants, were studied to determine the interaction between nematodes and NT fungi and arthrobotrisins, specific compounds produced by *A. oligospora* and other NT fungi that can impair trap formation (59, 60). In this study, AoMedA, AoBrlA, and AoAbaA played an important role in the biosynthesis of arthrobotrisins and other secondary metabolites; volcanic map analysis showed that a high number of compounds were downregulated in mutant strains. There was no significant difference in the content of secondary metabolites between the Δ*AowetA* mutant and WT strain, whereas WetA has an important role in secondary metabolites in *Aspergillus* species (61, 62). Overall, AoMedA, AoBrlA, and AoAbaA play a vital role in the secondary metabolism of *A. oligospora*, and AoMedA is required for the biosynthesis of arthrobotrisins.

In this study, the roles of four key conidiation genes *AomedA*, *AobrlA*, *AoabaA*, and *AowetA* were characterized in *A. oligospora*, and these genes were essential for conidiation and trap formation and had pleiotropic roles in mycelial development, trap

formation, LD accumulation, vacuole assembly, and secondary metabolism (Fig. 10). Based on Y1H and RT-qPCR analyses, there are complex interactions between *AomedA* and three central regulatory genes. *AobrlA* regulates *AomedA*, *AoabaA*, and *AowetA* and *AomedA* and *AoabaA* regulate *AowetA*; these genes are involved in multiple intracellular events, such as the number of septa and nuclei, lipid metabolism, vacuole assembly, autophagy, peroxisome, endocytosis, and secondary metabolism. In conidiation, AoBrlA is required for the development of conidiophores. AoAbaA is indispensable for forming conidia and AoMedA and AoWetA are necessary for conidia morphology and conidia yield. Interestingly, AoMedA is indispensable for trap formation, whereas three central regulators play a negative role in trap formation. In summary, our study first elaborated

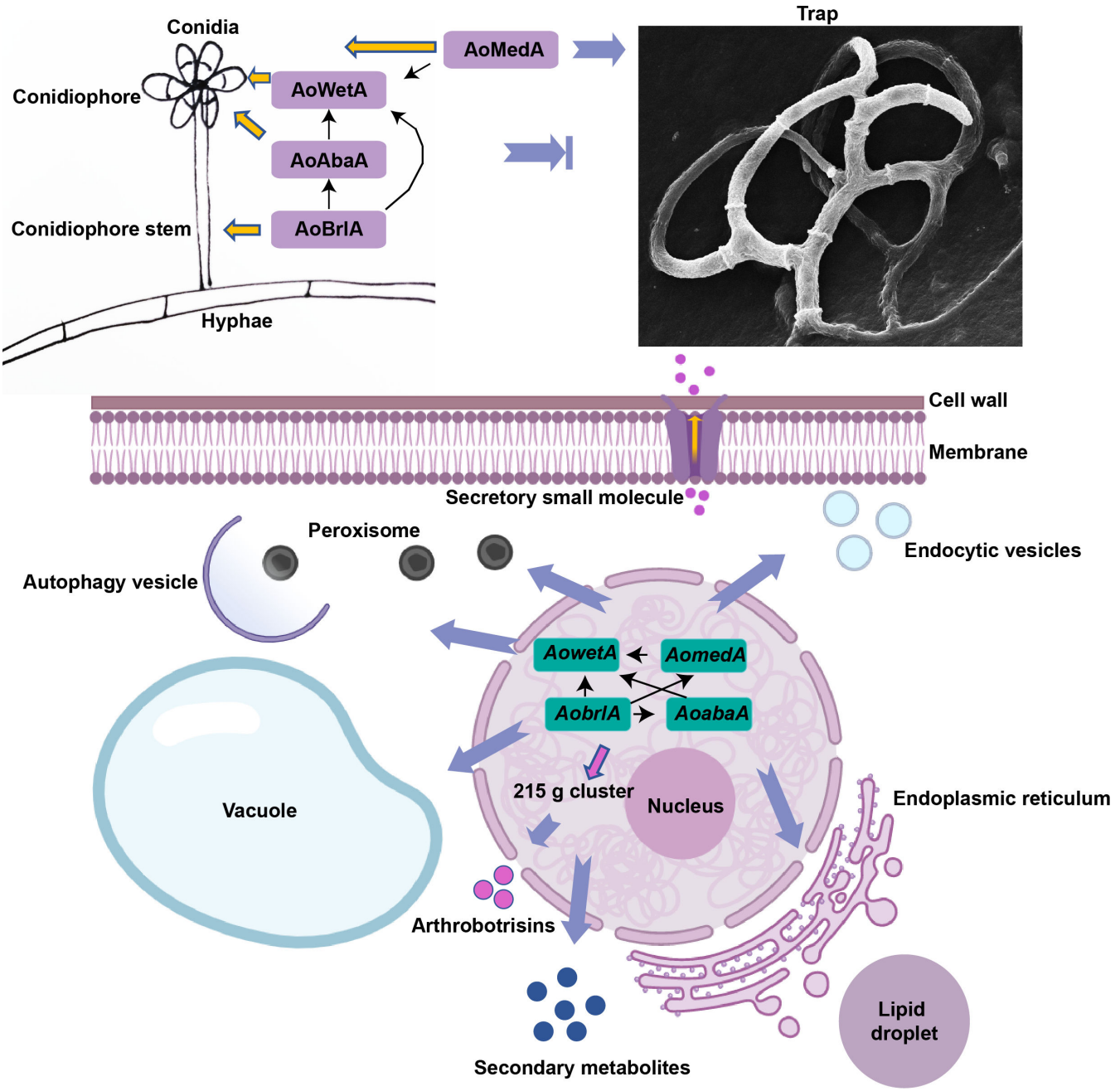

FIG 10 proposed model for the regulation of AoMedA, AoBrlA, AoAbaA, and AoWetA in *A. oligospora*. In this model, complex interactions between *AomedA* and three central regulatory genes (*AobrlA*, *AoabaA*, and *AowetA*) are illustrated; they are required for conidiation and trap formation and play a varied role in cell septa, nuclei, lipid metabolism, vacuole assembly, autophagy, endocytosis, and secondary metabolism.

the functions and regulatory mechanism of *AomedA* and three central regulatory genes in mycelial growth, development, and differentiation of the NT fungus *A. oligospora*, provided a broad basis for elucidating the molecular mechanism of conidiation, and outlined the regulatory relationship between conidiation and trap formation in NT fungi.

MATERIALS AND METHODS

Strains and culture conditions

A. oligospora (ATCC24927) WT and derived mutant strains were incubated on PDA, TG, TYGA, and corn dextrose with yeast extract (CMY) at 28°C for determining mycelial growth and conidia (63). *Saccharomyces cerevisiae* (FY834) and *Escherichia coli* strain DH5α were used for constructing the knockout vectors, as previously described (64). *Caenorhabditis elegans* (strain N2) was cultured on an oatmeal medium at 26°C and used for trap induction (27).

Sequence analysis of AoMedA, AoBrlA, AoAbaA, and AoWetA

The orthologous AomedA (AOL_s00210g120), AobrlA (AOL_s00097g514), AoabaA (AOL_s00080g63), and AowetA (AOL_s00173g221) were identified from *A. oligospora* using the orthologs of *A. nidulans* as a query. Their orthologous sequences from different fungi were blasted, and the biochemical properties of proteins were analyzed by the ProtParam tool (https://web.expasy.org/protparam/). DNAman software package (Version 5.2.2) was used to align different sequences and analyze their similarity, and a neighbor-joining tree was constructed by the MEGA 5 software package (65).

Deletion of *AomedA*, *AobrlA*, *AoabaA*, and *AowetA*

The disruption of *AomedA*, *AobrlA*, *AoabaA*, and *AowetA* was performed using a modified yeast cloning procedure, as previously described (66, 67). *A. oligospora* genome DNA was used as a template for amplifying the 5′- and 3′-flanking sequences of these genes, and the *hph* cassette was amplified from pCSN44, the paired primers listed in Table 2. The plasmid of pRS426 was used to construct the corresponding knockout vectors pRS426-AomedA-hph, pRS426-AobrlA-hph, pRS426-AoabaA-hph, and pRS426-AowetA-hph. The disruption sequences were transformed into *A. oligospora* protoplasts, as previously described (54). Positive transformants were confirmed via PCR and Southern blotting, as described previously (54, 68).

Analysis of mycelial growth, conidiation, and stress tolerance

WT and mutant strains were cultured on PDA and TG medium for 5 d for observing mycelial growth, colony morphology, and aerial hyphae, and the colony diameters were recorded at 24-h intervals. To observe the morphology of cell nuclei, LDs, and vacuole, 10 μg/mL of CFW (Sigma Aldrich), DAPI (Sigma-Aldrich), BODIPY (Sigma-Aldrich), and CMAC (Sigma-Aldrich) dyes were used to stain the mycelia (69, 70). The mycelia were examined by TEM.

To analyze sporulation, CMY medium was used to cultivate the fungal strains, and the mycelium was transferred to the slide for observing the conidiophore structures by light microscopy and SEM (71). Meanwhile, the conidia were washed with sterile water; hyphae were filtered for collecting conidia and observed via light microscopy and TEM; conidia were stained with CFW and observed by fluorescence electron microscopy.

The stress response of fungal strains to chemical reagents was performed, as described previously (64). In addition, to induce temperature stress, plates coated with 10,000 conidia were incubated on TG medium at 28, 30, 37, and 42°C for 30 min, 42°C for 1 h, and 50°C for 10 min and cultured at 28°C until 24 h and at 28°C for 30 min as control. RGI values of the strains were calculated, as previously described (72, 73).

Analysis of trap formation and pathogenicity

Mycelial discs (6 mm) of WT and mutant strains were incubated on a WA plate at 28°C for 4 d. Approximately 200 nematodes were added to each plate for trap induction. The number of traps and captured nematodes were counted and imuntaaged at 12-h intervals, and the ultrastructure of the trap cells was observed by TEM.

Observation of hyphal autophagy and western blot analysis

WT and mutant strains were inoculated in TYGA for 5 d, then mycelial samples were stained with MDC (100 μg/mL) for 30 min at 37°C, and observed by fluorescence electron microscopy.

WT and mutant strains were inoculated in potato dextrose liquid medium for 3 d at 28°C and 180 rpm, hyphae were collected, total protein was extracted by liquid nitrogen grinding using radioimmunoprecipitation assay lysis buffer, the concentration of total proteins was calculated using a bicinchoninic acid (BCA) protein assay reagent (Beijing Dingguochangsheng Biotechnology, China), and 50 μg of proteins was loaded into each well for Western blot analysis with anti-SQSTM1/p62, anti-Pex5/PER3, and anti-Pex7 antibodies (Abcam, Cambridge, UK), which diluted 1,000 times with primary antibody dilution buffer, and β-tubulin (Beyotime, Shanghai, China) as control. Antibody binding was visualized using an ECL Plus Western blotting detection reagent (Amersham Biosciences) after binding to a horseradish peroxidase-conjugated secondary antibody (74).

Transcriptome sequencing and RT-qPCR analyses

The WT, Δ*AomedA*, and Δ*AowetA* mutant strains were cultured on CMY medium with cellophane at 28°C for 5 d, and the mycelia were collected and three independent biological replicates were used for each sample. The samples were sent to Shanghai Meiji Biological Company (Shanghai, China) for RNA sequencing, and the RNA-Seq data were analyzed through the OmicShare online platform (www.majorbio.com). DEGs were identified based on the thresholds of $|\log2 \text{ ratio}| \geq 1$ and adjusted $P < 0.05$.

The Axygen kit procedure (Axygen Biotech Company, Hangzhou, China) was used for total RNA extraction of WT and mutant strains, which were cultured on CMY at 28°C for 5 d. To verify the accuracy of transcriptome data, several genes associated with endocytosis, phagosome, lipid metabolism, cell growth, and peroxisome were selected, and their transcript levels were determined by RT-qPCR analysis, as previously described (23). All primers used for RT-qPCR are listed in Table 3. The relative transcription level (RTL) of each gene was calculated as the ratio of the transcription level between mutant and WT strain according to the $2^{-\Delta\Delta Ct}$ method (75), and the β-tubulin gene (AOL_s00076g640) was used as an internal standard.

Y1H assay

The association of a transcription factor with a ~1,000 bp DNA fragment (putative promoter region of a gene) was assayed by Y1H according to the Matchmaker Gold Y1H Library Screening System User Manual (Clontech, USA). The promoter region with a ~1,000 bp DNA fragment (*AomedA*, *AoabaA*, and *AowetA*) was cloned into the pAbAi vector. The plasmids (pAbAi-AoMedA, pAbAi-AoAbaA, and pAbAi-AoWetA) were linearized and cloned into *S. cerevisiae* Y1HGold cells (TaKaRa, Dalian, China) as bait plasmids. Then, the cDNA sequence of *AomedA*, *AobrlA*, and *AoabaA* was cloned into a pGADT7 vector. The recombinant plasmids pGADT7-AoMedA, pGADT7-AoBrlA, and pGADT7-AoAbaA were further transformed into the Y1H1baitGold (pAbAi-AoMedA, pAbAi-AoAbaA, and pAbAi-AoWetA) strain. The transformed cells were plated on an SD/-Ura and SD/-Leu agar medium with 600 ng/mL aureobasidin A to identify the interactions between them. SD/-Ura and SD/-Leu agar medium without aureobasidin A was used as a control; pGADT7-Rec-p53/p53-AbAi as a positive control; and

TABLE 3 Primers used for RT-qPCR analysis

Primers	Sequence (5′–3′)	Primers	Sequence (5′–3′)
54g700 F	CAAACCACCCACCACCAAAT	215g893 F	ATACCGCCAACACCCTCTAC
54g700 R	GGATGGACAGGAGAAGGACC	215g893 R	AACCATCTTCATCTCGGCCT
83g487 F	TTCTCTTCGTCCCAAGCCAC	83g25 F	AGCTCCCGAAACGAGTCTAA
83g487 F	ACCGGTTCGAGTGGAGTCTA	83g25 R	ATTGATCATGTGATTATCCT
169g18 F	AAGCTACACCCAATCAACGC	80g93 F	CCAGGGTCGTCAGTATCTT
169g18 R	TTGCGATGCTGACGATCTTG	80g93 R	CAGCATCTTCCAGGTCAA
215g516 F	TTCAAACGCAGCTCCTTCAC	54g811 F	ATTCCGCAACTTCTCCCTCA
215g516 R	AAGCGGGTTGACAGATGAGA	54g811 R	GGCATGTTTGGATTCTGGGG
75g211 F	ATTACGGCCGCCTAGTAGTC	80g63 F	AACTTTATGCGCCTTGTCGT
75g211 R	CTCGTTTGGACCTGGTTGTG	80g63 R	TTGGCTAGGTGGTCTGTACG
173g221 F	TTACATGCCACCCCAAGTCC	43g361 F	GATTCCAGTCCCGTGAATTC
173g221 R	CAATTGCAACTGCGTCCACA	43g361 R	GCTAAGGAGAGGATGGGCAT
7g157 F	CTCTCCGGCAAAGACAATCG	97g514 F	TTGAGGCCTCGATCCGTAGA
7g157 R	GTCGACTGAGGATAGTAGCT	97g514 R	AGGTAGATGGCGCTGTTACG
6g570 F	GCGGATCCAACATGAAGCTT	210g120 F	TCCGGCCCAATGATTCAGAA
6g570 R	GGTTGACAACTGGGATGCTG	210g120 R	AGATCGCAGGAACATGGTGA-3
97g317 F	GAATGTGAGGGTGGCGAAGA	54g737 F	CATCTCTTCGCCAACCCACC
97g317 R	TAGCACGAACCCATGAACGG	54g737 R	TTCTTTGTCGGCTCATCGGG
110g119 F	GCCTGCGTCGTTAGTGTTTT	4g362 F	CTTCCTTGCCCTTCACCCAA
110g119 R	ACCCTTGCCTGCTGAAGAAT	4g362 R	TTCTTGAGGCTACCGTCGTG
193g4 F	ACCGGCAATCAACCTGTCTT	79g361 F	GCGAACTACCCAACAGACCA
193g4 R	CGCAAGCTCTCCGATCTCAT	79g361 R	TGACCTTGTAACGCCGGATT
79g276 F	GGATGTGGGCCGGTATTAGG	83g431 F	ATTGGATCCGGACATGTGCTT
79g276 R	CTACAACTGCGACCGTCCTT	83g431 R	GCCATTTGCGCTTTGAAGGA
112g52 F	CTGCCGGTCCTCACTTCAAC	215g205 F	GCCTTCGAGAATGCCAATGT
112g52 R	CAACAACAGTTCGTCCGAGG	215g205 R	CCGCGGGTTCTCAAGAGTAG
75g201 F	TTCCCTGCAATCAATTCGGC	78g492 F	ATCCAGCTGTTCCATTCCCG
75g201 R	GCTTCATACCCAACAAACCCG	78g492 R	ACGGCTTTGGTATTGGCTTC
210g359 F	AACCTGGCCTCGTCAAGAAG	97g208 F	CCCCCGCATAAGGACATTCA
210g359 R	GTGGGTGTAGGTGCGAAGAG	97g208 R	GTAGAAGCGCCACATCAAGC
54g368 F	AAGTTCGTCCACGCCAAGAA	97g207 F	ATCCTCCAACAAGACGTCGC
54g368 R	CCAACTGGCGCTACAGGTTT	97g207 R	TCTCCTCCGACCGTTTTTCG
78g71 F	ACCACTCCCAATTACCGCAG	117g35 F	CTTCGCTCAAATGCTCGTCG
78g71 R	TCGGTGTGATCCTCGCTCTA	117g35 R	TAGAAGCACCCGTAACCCCT
80g44 F	TTCGCGGATGGTGGAGATTT	215g336 F	TCTCCGTCGCACCCCTATTA
80g44 R	GCAAAACCAAAGTCGGCGAT	215g336 R	TCTCCGTCGCACCCCTATTA
83g233 F	TTCGGTCAAAAGGCGCAATG	97g364 F	CAAATTCCCAGCCGGCAAAA
83g233 R	GCTAACGATAAGGTCCCGCA	97g364 R	CGGCGAATAAGACTGGCTCT
78g27 F	ACAGGCGGTGTACAGTCTTC	83g260 F	AGGGTGGTGAGCGAAGATTG
78g27 R	CGAATTTCCCGAGCGAACTG	83g260 R	GGAACCGTCTCGTTTTTGGC
43g730 F	ATACCTTCTTGCTCACCCCG	83g512 F	ATCCGCCAATTCAAACGCAC
43g730 R	GCTTCGTTGAACTTGTCGGC	83g512 R	TCTCTGAACAATGGACCGGC
173g374 F	TCATCAACAAGACCGGCGAA	4g606 F	GTCGCCAGCTACACAAATGC
173g374 R	GGCTTCCTTTGGTGTCATGG	4g606 R	AAGCGTGTGAGATCAGTCGT
54g687 F	CACCAAACCTATGTCAACGGC	4g235 F	ACTTTTGGCTCTGGACCTCG
54g687 R	GCCTCGCTCAACTTACCACT	4g235 R	CCTGGGCAGCTTGTTCGATA
4g133 F	ACTCGTGACCAACTTACCCG	6g253 F	AAGTTTAGGGATCGGTGCGG
4g133 R	CTAGCAACGATCAGACGGGG	6g253 R	CCTCAGGGTCGCTATCATCG
6g411 F	TCACAGATAACTACGGCGGC	109g23 F	CATTCAGCACACCGGTTCTC
6g411 R	CTGTTTCCCCAGCATATCCCA	109g23 R	CGAGCGGTCTGGATGTCAAT
78g58 F	GTTCCTTCGCAGTTCCCTCA	81g328 F	AGAGCGGAAACCTAGACATCA
78g58 R	ACCGGTAGCTTGTTGGTTGA	81g328 R	TTAGGTTGCCTTCGGTTCGG

(*Continued on next page*)

TABLE 3 Primers used for RT-qPCR analysis (*Continued*)

Primers	Sequence (5′–3′)	Primers	Sequence (5′–3′)
75g198 F	TCAAACCTGCCGACGAACTA	75g194 F	TCACCGCGCAATCAGTCTAA
75g198 R	GGGTGGCCTGTTCTAACTCG	75g194 R	GAAGGGGAACGGTTCTTGGA
6g248 F	GATCCCGAGCTCCAATACCC	75g120 F	GTCATGGACGTTTCGGGGAT
6g248 R	AATGCAAGTCCTTTCCAGCG	75g120 R	TTGTGGAATGTTAGCCGGGA
215g255 F	TCCACCCGTATCCCCAAGAT	173g67 F	CCCAGCTAGACCCTCCATTG
215g255 R	GAGAGAGGAGCAACGTCGAG	173g67 R	AATCTCCCTGGTCAACTCGC
78g38 F	ACAGACAATGTTCGAGCGGT	78g181 F	ACAAAGTCGCCGTCAGAGAG
78g38 R	CTTCCGAGAGCTGACCCATT	78g181 R	CCGTCAGTTCGTTGGGAGTT
188g58 F	CCGTCTTCCCAGTTCTCGTC	4g330 F	TTCGAAGTCGTCATCTCCCG
188g58 R	AGCCATCATTGATACCGCGT	4g330 R	TCGCTGTCTTTTTCTCGGGG
6g247 F	CCAGTGCGAAGACAGGACAT	43g133 F	GCAACAAATCGGCCTAACGG
6g247 R	GCACAACCGTCCTTGTTTGT	43g133 R	CTGTTCGCCCAGCTAGTGAT
78g47 F	AATGTTACCGCAGCTCCCTC	78g126 F	GGCGTTCCAAAATCAGTTCCA
78g47 R	TGACCGTAAGCATGCTCGAA	78g126 R	GTCTCGCCGGTTTCACTAGG
54g446 F	GTAGCCTTCTATCGCGGTGC	76g160 F	GCGATGTGGCTGAATAACGG
54g446 R	TGCCTCTTTCCATCGTCCAC	76g160 R	ACAACCGAATCTCCACCACC
159g2 F	TCACCGGACAGAGGGTTTTG	54g253 F	AGAAATACAAGGGGACGGCG
159g2 R	CAAGACTTCCGCCATCTCGT	54g253 R	GGGACTCCGTGACAATAGCA
215g358 F	CATATGCCAAGGAAGCCGGT	43g20 F	TTGGACCGCACATACTAGCC
215g358 R	TTAGGTTGGCGGTTTGAGGT	43g20 R	CGTCTTATTCTCTGCGCGTG
188g92 F	CCGCCTTTCATCCCTCGAAT	54g312 F	GACAAGACCAAGGCCGAAGT
188g92 R	TGCGAATCCTTCTTTGTCCCA	54g312 R	CCGGTGCAGGAGTTGATGTA
76g585 F	ATCCTCAAACCTTCCCTCGC	76g229 F	AGCGATGGGAATGTGGTTGA
76g585 R	ACCGCTTCTGATCTCTGTGG	76g229 R	GTACTTCGCGGAACAAACCC
97g406 F	CTCCAACAATGAGGCCGAGA	97g406 F	GGGCTGCGGACAAGGATAAA
76g640 F	CCACCTTCGTCGGTAACTC	76g640 R	TCGTCCATACCCTCACCAG

pABAI-AoMedA, pABAI-AoAbaA, and pABAI-AoWetA plus pGADT7 as negative controls (76). All primers used for the Y1H assay are listed in Table 4.

Y2H assay

The cDNA of *A. oligospora* was obtained as aforementioned, and then the cDNA sequences of *AomedA* and AOL_s00054g434 were amplified using the paired primers (Table 4). The cDNA sequence of *AomedA* was cloned into pGADT-7, and the cDNA sequence of AOL_s00054g434 was cloned into pGBKT-7. The Y2H assay was performed as previously described (64).

UPLC-MS analysis assay

WT and mutant strains were inoculated into PD broth at 28°C and 180 rpm for 6 d, and the fermentation broth was then extracted using ethyl acetate and dried under vacuum (64, 69). The samples were dissolved in methanol and analyzed by LC-MS using the Thermo Scientific Dionex Ultimate 3000 UHPLC system with a Thermo high-resolution Q Exactive focus mass spectrometer (Thermo, Bremen, Germany). Compounds Discoverer 3.0 software (Thermo Fisher Scientific, CA, USA) was used for untargeted metabolomics analysis.

Statistical analysis

Prism 8.0 (GraphPad Software, San Diego, CA, USA) was used as the tool for statistical analysis, with one-way ANOVA followed by Tukey's honestly significant difference test being performed with $P < 0.05$ considered as statistically significant. All experiments were repeated three times.

TABLE 4 Primers used for Y1H and Y2H assays

Primers	Sequence (5′–3′)	Description
AD-AoMedA F	ATATGGCCATGGAGGCCAGTATGGCAGCCTCCTACACCAA	Connected to pGADT7 vector
AD-AoMedA R	TATCGATGCCCACCCGGGTGGGACATCGAGTAGGTGTTGT	
AD-AoBrlA F	ATATGGCCATGGAGGCCAGTATGTCCCATCATAACATTCA	
AD-AoBrlA R	TATCGATGCCCACCCGGGTGATTTTCAAGCTTGATCCCCG	
AD-AoAbaA F	ATATGGCCATGGAGGCCAGTATGAGGAGCAGAACAAAGTC	
AD-AoAbaA R	TATCGATGCCCACCCGGGTGCTGCATATTGCCCATCCCAC	
ABI-AoMedA F	TTGAATTCGAGCTCGGTACCGATGAGAGATGGATGGTTTG	Connected to pABAI vector
ABI-AoMedA R	TCGACAGATCCCCGGGTACCGTTGCTGAGAGCCTGGGTGT	
ABI-AoAbaA F	TTGAATTCGAGCTCGGTACCCCGCATCGAGCAGAGAATTT	
ABI-AoAbaA R	TCGACAGATCCCCGGGTACCATTTGGGGATGATGTATATC	
ABI-AoWetA F	TTGAATTCGAGCTCGGTACCTAGGAAATTTCGCTGCATCG	
ABI-AoWetA R	TCGACAGATCCCCGGGTACCTTGAACTCAAGTTGCCCGGA	
AD-AoMedA F	ATATGGCCATGGAGGCCAGTATGGCAGCCTCCTACACCAA	Connected to pGADT7 vector
AD-AoMedA R	TATCGATGCCCACCCGGGTGGGACATCGAGTAGGTGTTGT	
BD-54g434 F	TGCATATGGCCATGGAGGCCATGGCTGCCGTTGCAAAACA	Connected to pGBKT7 vector
BD-54g434 R	GCAGGTCGACGGATCCCCGGGTCGTAAGCAGGTGGAGATG	

ACKNOWLEDGMENTS

We are grateful to the Microbial Library of the Germplasm Bank of Wild Species from Southwest China for preserving and providing experimental strains, and to Guo Ying-qi (Kunming Institute of `Zoology, Chinese Academy of Sciences) for her help with taking and analyzing TEM images.

Funding for this study was provided by the National Natural Science Foundation of China (grant 31960556), the Special Fund of the Yunnan University "double first-class" Construction, and Applied Basic Research Foundation of Yunnan Province (grant nos. 202201BC070004, 202001BB050004).

K.-Q.Z. and J.Y. conceived and designed the study. N.B. performed the experiments. N.B., M.X., Q.L., Y.Z., and X.Y. analyzed the data. N.B. and J.Y. contributed to manuscript preparation and revision. All authors read and approved the final manuscript.

We declare that we have no conflicts of interests.

AUTHOR AFFILIATIONS

[1]State Key Laboratory for Conservation and Utilization of Bio-Resources & Key Laboratory for Microbial Resources of the Ministry of Education, School of Life Sciences, Yunnan University, Kunming, China
[2]School of Life Sciences, Yunnan University, Kunming, China
[3]School of Resource, Environment and Chemistry, Chuxiong Normal University, Chuxiong, China

AUTHOR ORCIDs

Jinkui Yang http://orcid.org/0000-0002-3106-2189

FUNDING

Funder	Grant(s)	Author(s)
MOST | National Natural Science Foundation of China (NSFC)	31960556	Jinkui Yang
云南省科学技术厅 | Applied Basic Research Foundation of Yunnan Province (Yunnan Province Applied and Basic Research Foundation)	202001BB050004, 202201BC070004	Ke-Qin Zhang

AUTHOR CONTRIBUTIONS

Na Bai, Formal analysis, Investigation, Methodology, Writing – original draft | Meihua Xie, Data curation, Resources, Software, Validation | Qianqian Liu, Resources, Software, Validation | Yingmei Zhu, Resources, Software, Validation | Xuewei Yang, Formal analysis, Resources, Software | Ke-Qin Zhang, Funding acquisition, Project administration | Jinkui Yang, Conceptualization, Funding acquisition, Supervision, Writing – review and editing

DATA AVAILABILITY

The data that support the findings of this study are included in the paper and the associated Supplementary Materials. All the RNA-seq data of this study have been deposited in the Gene Expression Omnibus database under accession number GSE230299.

ADDITIONAL FILES

The following material is available online.

Supplemental Material

Supplemental figures and tables (AEM00983-23- S0001.docx). Figure S1-S8; Table S1.

REFERENCES

1. Nieuwenhuis BPS, James TY. 2016. The frequency of sex in fungi. Philos Trans R Soc Lond B Biol Sci 371:20150540. https://doi.org/10.1098/rstb.2015.0540
2. Jung B, Kim S, Lee J. 2014. Microcycle conidiation in filamentous fungi. Mycobiology 42:1–5. https://doi.org/10.5941/MYCO.2014.42.1.1
3. Yuan BH, Li H, Liu L, Du XH. 2021. Successful induction and recognition of conidiation, conidial germination and chlamydospore formation in pure culture of *Morchella*. Fungal Biol 125:285–293. https://doi.org/10.1016/j.funbio.2020.11.005
4. Park HS, Yu JH. 2012. genetic control of asexual sporulation in filamentous fungi. Curr Opin Microbiol 15:669–677. https://doi.org/10.1016/j.mib.2012.09.006
5. Mirabito PM, Adams TH, Timberlake WE. 1989. Interactions of three sequentially expressed genes control temporal and spatial specificity in *Aspergillus* development. Cell 57:859–868. https://doi.org/10.1016/0092-8674(89)90800-3
6. Al Abdallah Q, Choe SI, Campoli P, Baptista S, Gravelat FN, Lee MJ, Sheppard DC. 2012. A conserved C-terminal domain of the *Aspergillus fumigatus* developmental regulator meda is required for nuclear localization, adhesion and virulence. PLoS One 7:e49959. https://doi.org/10.1371/journal.pone.0049959
7. Krijgsheld P, Bleichrodt R, van Veluw GJ, Wang F, Müller WH, Dijksterhuis J, Wösten HAB. 2013. Development in *Aspergillus*. Stud Mycol 74:1–29. https://doi.org/10.3114/sim0006
8. Etxebeste O, Garzia A, Espeso EA, Ugalde U. 2010. *Aspergillus nidulans* asexual development: making the most of cellular modules. Trends Microbiol 18:569–576. https://doi.org/10.1016/j.tim.2010.09.007
9. Prade RA, Timberlake WE. 1993. The *Aspergillus Nidulans* brlA regulatory locus consists of overlapping transcription units that are individually required for conidiophore development. EMBO J 12:2439–2447. https://doi.org/10.1002/j.1460-2075.1993.tb05898.x
10. Adams TH, Wieser JK, Yu JH. 1998. Asexual sporulation in *Aspergillus nidulans*. Microbiol Mol Biol Rev 62:35–54. https://doi.org/10.1128/MMBR.62.1.35-54.1998
11. Tao L, Yu JH. 2011. Abaa and WetA govern distinct stages of *Aspergillus fumigatus* development. Microbiology (Reading) 157:313–326. https://doi.org/10.1099/mic.0.044271-0
12. Qin Y, Bao L, Gao M, Chen M, Lei Y, Liu G, Qu Y. 2013. *Penicillium decumbens* BrlA extensively regulates secondary metabolism and functionally associates with the expression of cellulase genes. Appl Microbiol Biotechnol 97:10453–10467. https://doi.org/10.1007/s00253-013-5273-3
13. Wang M, Sun X, Zhu C, Xu Q, Ruan R, Yu D, Li H. 2015. Pdbrla, PdabaA and PdwetA control distinct stages of conidiogenesis in *Penicillium digitatum*. Res Microbiol 166:56–65. https://doi.org/10.1016/j.resmic.2014.12.003
14. Ohara T, Inoue I, Namiki F, Kunoh H, Tsuge T. 2004. Ren1 is required for development of microconidia and macroconidia, but not of chlamydospores, in the plant pathogenic fungus *Fusarium oxysporum*. Genetics 166:113–124. https://doi.org/10.1534/genetics.166.1.113
15. Lau GW, Hamer JE. 1998. Acropetal: a genetic locus required for conidiophore architecture and pathogenicity in the rice blast fungus. Fungal Genet Biol 24:228–239. https://doi.org/10.1006/fgbi.1998.1053
16. Zhang AX, Mouhoumed AZ, Tong SM, Ying SH, Feng MG. 2019. BrlA and AbaA govern virulence-required dimorphic switch, conidiation, and pathogenicity in a fungal insect pathogen. mSystems 4:e00140-19. https://doi.org/10.1128/mSystems.00140-19
17. Li F, Shi HQ, Ying SH, Feng MG. 2015. WetA and VosA are distinct regulators of conidiation capacity, conidial quality, and biological control potential of a fungal insect pathogen. Appl Microbiol Biotechnol 99:10069–10081. https://doi.org/10.1007/s00253-015-6823-7
18. Zeng G, Chen X, Zhang X, Zhang Q, Xu C, Mi W, Guo N, Zhao H, You Y, Dryburgh F-J, Bidochka MJ, St Leger RJ, Zhang L, Fang W. 2017. Genome-wide identification of pathogenicity, conidiation and colony sectorization genes in *Metarhizium Robertsii*. Environ Microbiol 19:3896–3908. https://doi.org/10.1111/1462-2920.13777
19. Ji X, Yu Z, Yang J, Xu J, Zhang Y, Liu S, Zou C, Li J, Liang L, Zhang KQ. 2020. Expansion of adhesion genes drives pathogenic adaptation of nematode-trapping fungi. iScience 23:101057. https://doi.org/10.1016/j.isci.2020.101057
20. Zhu MC, Li XM, Zhao N, Yang L, Zhang KQ, Yang JK. 2022. Regulatory mechanism of trap formation in the nematode-trapping fungi. JoF 8:406. https://doi.org/10.3390/jof8040406
21. Yang J, Wang L, Ji X, Feng Y, Li X, Zou C, Xu J, Ren Y, Mi Q, Wu J, Liu S, Liu Y, Huang X, Wang H, Niu X, Li J, Liang L, Luo Y, Ji K, Zhou W, Yu Z, Li G, Liu Y, Li L, Qiao M, Feng L, Zhang K-Q, Andrianopoulos A. 2011. Genomic and Proteomic analyses of the fungus *Arthrobotrys oligospora* provide insights into Nematode-trap formation. PLoS Pathog 7:e1002179. https://doi.org/10.1371/journal.ppat.1002179
22. Yang C-T, Vidal-Diez de Ulzurrun G, Gonçalves AP, Lin H-C, Chang C-W, Huang T-Y, Chen S-A, Lai C-K, Tsai IJ, Schroeder FC, Stajich JE, Hsueh Y-P. 2020. Natural diversity in the predatory behavior facilitates the establishment of a robust model strain for nematode-trapping fungi. Proc Natl Acad Sci U S A 117:6762–6770. https://doi.org/10.1073/pnas.1919726117

23. Bai N, Zhang G, Wang W, Feng H, Yang X, Zheng Y, Yang L, Xie M, Zhang KQ, Yang J. 2022. Ric8 acts as a regulator of G-protein signalling required for nematode-trapping lifecycle of *Arthrobotrys oligospora*. Environ Microbiol 24:1714–1730. https://doi.org/10.1111/1462-2920.15735
24. Ma N, Zhao Y, Wang Y, Yang L, Li D, Yang J, Jiang K, Zhang K-Q, Yang J. 2021. Functional analysis of seven regulators of G protein signaling (RGSs) in the nematode-trapping fungus *Arthrobotrys oligospora*. Virulence 12:1825–1840. https://doi.org/10.1080/21505594.2021.1948667
25. Chen SA, Lin HC, Schroeder FC, Hsueh YP. 2021. Prey sensing and response in a nematode-trapping fungus is governed by the MAPK pheromone response pathway. Genetics 217:iyaa008. https://doi.org/10.1093/genetics/iyaa008
26. Xie M, Bai N, Yang J, Jiang K, Zhou D, Zhao Y, Li D, Niu X, Zhang K-Q, Yang J. 2019. Protein kinase Ime2 is required for mycelial growth, conidiation, osmoregulation, and pathogenicity in nematode-trapping fungus *Arthrobotrys Oligospora*. Front Microbiol 10:3065. https://doi.org/10.3389/fmicb.2019.03065
27. Xie M, Yang J, Jiang K, Bai N, Zhu M, Zhu Y, Zhang KQ, Yang J. 2021. AoBck1 and AoMkk1 are necessary to maintain cell wall integrity, vegetative growth, conidiation, stress resistance, and pathogenicity in the nematode-trapping fungus *Arthrobotrys oligospora*. Front. Microbiol 12:649582. https://doi.org/10.3389/fmicb.2021.649582
28. Zhen Z, Xing X, Xie M, Yang L, Yang X, Zheng Y, Chen Y, Ma N, Li Q, Zhang KQ, Yang J. 2018. MAP kinase Slt2 orthologs play similar roles in conidiation, trap formation, and pathogenicity in two nematode-trapping fungi. Fungal Genet Biol 116:42–50. https://doi.org/10.1016/j.fgb.2018.04.011
29. Yang L, Li X, Xie M, Bai N, Yang J, Jiang K, Zhang KQ, Yang J. 2021. Pleiotropic roles of Ras GTPases in the nematode-trapping fungus *Arthrobotrys oligospora* identified through multi-Omics analyses. iScience 24:102820. https://doi.org/10.1016/j.isci.2021.102820
30. Yang L, Li X, Bai N, Yang X, Zhang K-Q, Yang J. 2022. Transcriptomic analysis reveals that Rho GTPases regulate trap development and lifestyle transition of the nematode-trapping fungus *Arthrobotrys oligospora*. Microbiol Spectr 10:e0175921. https://doi.org/10.1128/spectrum.01759-21
31. Ma Y, Yang X, Xie M, Zhang G, Yang L, Bai N, Zhao Y, Li D, Zhang KQ, Yang J. 2020. The Arf-GAP AoGlo3 regulates conidiation, endocytosis, and pathogenicity in the nematode-trapping fungus *Arthrobotrys oligospora*. Fungal Genet Biol 138:103352. https://doi.org/10.1016/j.fgb.2020.103352
32. Zhou D, Zhu Y, Bai N, Xie M, Zhang KQ, Yang J. 2021. Aolatg1 and Aolatg13 regulate autophagy and play different roles in conidiation, trap formation, and pathogenicity in the nematode-trapping fungus *Arthrobotrys oligospora*. Front Cell Infect Microbiol 11:824407. https://doi.org/10.3389/fcimb.2021.824407
33. Li X, Zhu M, Liu Y, Yang L, Yang J. 2023. Aoatg11 and Aoatg33 are indispensable for mitophagy, and contribute to conidiation, the stress response, and pathogenicity in the nematode-trapping fungus *Arthrobotrys oligospora*. Microbiol Res 266:127252. https://doi.org/10.1016/j.micres.2022.127252
34. Liu Q, Li D, Jiang K, Zhang KQ, Yang J. 2022. Aopex1 and Aopex6 are required for mycelial growth, conidiation, stress response, fatty acid utilization, and trap formation in *Arthrobotrys oligospora*. Microbiol Spectr 10:e0027522. https://doi.org/10.1128/spectrum.00275-22
35. Liu Q, Li D, Bai N, Zhu Y, Yang J. 2023. Peroxin Pex14/17 is required for trap formation, and plays pleiotropic roles in mycelial development, stress response, and secondary metabolism in *Arthrobotrys oligospora*. mSphere 8:e0001223. https://doi.org/10.1128/msphere.00012-23
36. Zhang G, Zheng Y, Ma Y, Yang L, Xie M, Zhou D, Niu X, Zhang KQ, Yang J. 2019. The velvet proteins vosa and velb play different roles in conidiation, trap formation, and pathogenicity in the nematode-trapping fungus *Arthrobotrys Oligospora* Front Microbiol 10:1917. https://doi.org/10.3389/fmicb.2019.01917
37. Lim YJ, Lee YH. 2020. F-box only and CUE proteins are crucial ubiquitination-associated components for conidiation and pathogenicity in the rice blast fungus, *Magnaporthe oryzae*. Fungal Genet Biol 144:103473. https://doi.org/10.1016/j.fgb.2020.103473
38. Li HX, Lu ZM, Zhu Q, Gong JS, Geng Y, Shi JS, Xu ZH, Ma YH. 2017. Comparative transcriptomic and proteomic analyses reveal a flug-mediated signaling pathway relating to Asexual sporulation of *Antrodia Camphorata*. Proteomics 17. https://doi.org/10.1002/pmic.201700256
39. Busby TM, Miller KY, Miller BL. 1996. Suppression and enhancement of the *Aspergillus nidulans* medusa mutation by altered dosage of the bristle and stunted genes. Genetics 143:155–163. https://doi.org/10.1093/genetics/143.1.155
40. Gravelat FN, Ejzykowicz DE, Chiang LY, Chabot JC, Urb M, Macdonald KD, al-Bader N, Filler SG, Sheppard DC. 2010. *Aspergillus fumigatus* meda governs adherence, host cell interactions and virulence. Cell Microbiol 12:473–488. https://doi.org/10.1111/j.1462-5822.2009.01408.x
41. Boylan MT, Mirabito PM, Willett CE, Zimmerman CR, Timberlake WE. 1987. Isolation and physical characterization of three essential conidiation genes from *Aspergillus nidulans*. Mol Cell Biol 7:3113–3118. https://doi.org/10.1128/mcb.7.9.3113-3118.1987
42. Yamada O, Lee BR, Gomi K, Iimura Y. 1999. Cloning and functional analysis of the *Aspergillus oryzae* conidiation regulator gene brlA by its disruption and Misscheduled expression. J Biosci Bioeng 87:424–429. https://doi.org/10.1016/s1389-1723(99)80089-9
43. Zhang JG, Xu SY, Ying SH, Feng MG. 2022. Roles of BrlA and AbaA in mediating asexual and insect pathogenic Lifecycles of *Metarhizium Robertsii*. J Fungi 8:1110. https://doi.org/10.3390/jof8101110
44. Jia L, Yu JH, Chen F, Chen W. 2021. Characterization of the asexual developmental genes brlA and wetA in Monascus ruber M7. Fungal Genet Biol 151:103564. https://doi.org/10.1016/j.fgb.2021.103564
45. Boni AC, Ambrósio DL, Cupertino FB, Montenegro-Montero A, Virgilio S, Freitas FZ, Corrocher FA, Gonçalves RD, Yang A, Weirauch MT, Hughes TR, Larrondo LF, Bertolini MC. 2018. *Neurospora crassa* developmental control mediated by the FLB-3 transcription factor. Fungal Biol 122:570–582. https://doi.org/10.1016/j.funbio.2018.01.004
46. Son H, Kim MG, Min K, Lim JY, Choi GJ, Kim JC, Chae SK, Lee YW. 2014. Weta is required for conidiogenesis and conidium maturation in the Ascomycete fungus *Fusarium graminearum*. Eukaryot Cell 13:87–98. https://doi.org/10.1128/EC.00220-13
47. Wu MY, Mead ME, Kim SC, Rokas A, Yu JH. 2017. Weta bridges cellular and chemical development in *Aspergillus flavus*. PLoS One 12:e0179571. https://doi.org/10.1371/journal.pone.0179571
48. Sigl C, Haas H, Specht T, Pfaller K, Kürnsteiner H, Zadra I. 2011. Among developmental regulators, StuA but not BrlA is essential for penicillin V production in *Penicillium chrysogenum*. Appl Environ Microbiol 77:972–982. https://doi.org/10.1128/AEM.01557-10
49. Kim KS, Lee YH. 2012. Gene expression profiling during conidiation in the rice blast pathogen *Magnaporthe oryzae*. PLoS One 7:e43202. https://doi.org/10.1371/journal.pone.0043202
50. Chacko N, Gold S. 2012. Deletion of the ustilago maydis ortholog of the *Aspergillus* sporulation regulator medA affects mating and virulence through pheromone response. Fungal Genet Biol 49(6):426–432.
51. Nishimura M, Hayashi N, Jwa NS, Lau GW, Hamer JE, Hasebe A. 2000. Insertion of the LINE retrotransposon MGL causes a conidiophore pattern mutation in *Magnaporthe grisea*. Mol Plant Microbe Interact 13:892–894. https://doi.org/10.1094/MPMI.2000.13.8.892
52. Son H, Kim MG, Min K, Seo YS, Lim JY, Choi GJ, Kim JC, Chae SK, Lee YW. 2013. AbaA regulates Conidiogenesis in the Ascomycete fungus *Fusarium graminearum*. PLoS One 8:e72915. https://doi.org/10.1371/journal.pone.0072915
53. Pandit R, Patel R, Patel N, Bhatt V, Joshi C, Singh PK, Kunjadia A. 2017. RNA-Seq reveals the molecular mechanism of trapping and killing of root-knot nematodes by nematode-trapping fungi. World J Microbiol Biotechnol 33:65. https://doi.org/10.1007/s11274-017-2232-7
54. Xie M, Ma N, Bai N, Yang L, Yang X, Zhang KQ, Yang J. 2022. PKC-Swi6 signaling regulates asexual development, cell wall integrity, stress response, and lifestyle transition in the nematode-trapping fungus *Arthrobotrys oligospora.* Sci China Life Sci 65:2455–2471. https://doi.org/10.1007/s11427-022-2118-0
55. Veenhuis M, Van Wijk C, Wyss U, Nordbring-Hertz B, Harder W. 1989. Significance of electron dense microbodies in trap cells of the nematophagous fungus *Arthrobotrys oligospora*. Antonie Van Leeuwenhoek 56:251–261. https://doi.org/10.1007/BF00418937
56. Zhou D, Zhu Y, Bai N, Yang L, Xie M, Yang J, Zhu M, Zhang KQ, Yang J. 2022. AoATG5 plays pleiotropic roles in vegetative growth, cell nucleus

development, conidiation, and virulence in the nematode-trapping fungus *Arthrobotrys oligospora*. Sci China Life Sci 65:412–425. https://doi.org/10.1007/s11427-020-1913-9
57. Birgisdottir ÅB, Johansen T. 2020. Autophagy and endocytosis - interconnections and interdependencies. J Cell Sci 133:10. https://doi.org/10.1242/jcs.228114
58. Morita T, Yamada T, Yamada S, Matsumoto K, Ohta K. 2011. Fission yeast ATF/CREB family protein Atf21 plays important roles in production of normal spores. Genes Cells 16:217–230. https://doi.org/10.1111/j.1365-2443.2010.01480.x
59. Yu X, Hu X, Pop M, Wernet N, Kirschhöfer F, Brenner-Weiß G, Keller J, Bunzel M, Fischer R. 2021. Fatal attraction of *Caenorhabditis elegans* to predatory fungi through 6-methyl-salicylic acid. Nat Commun 12. https://doi.org/10.1038/s41467-021-25535-1
60. He Z-Q, Tan J-L, Li N, Zhang H-X, Chen Y-H, Wang L-J, Zhang K-Q, Niu X-M. 2019. Sesquiterpenyl epoxy-cyclohexenoids and their signaling functions in nematode-trapping fungus *Arthrobotrys Oligospora*. J Agric Food Chem 67:13061–13072. https://doi.org/10.1021/acs.jafc.9b04968
61. Wu MY, Mead ME, Lee MK, Ostrem Loss EM, Kim SC, Rokas A, Yu JH. 2018. Systematic dissection of the evolutionarily conserved weta developmental regulator across a genus of filamentous fungi. mBio 9:e01130-18. https://doi.org/10.1128/mBio.01130-18
62. Wu MY, Mead ME, Lee MK, Neuhaus GF, Adpressa DA, Martien JI, Son YE, Moon H, Amador-Noguez D, Han KH, Rokas A, Loesgen S, Yu JH, Park HS. 2021. Transcriptomic, protein-DNA interaction, and metabolomic studies of vosa, velb, and weta in *Aspergillus Nidulans* asexual spores. mBio 12:e03128-20. https://doi.org/10.1128/mBio.03128-20
63. Yang X, Ma N, Yang L, Zheng Y, Zhen Z, Li Q, Xie M, Li J, Zhang KQ, Yang J. 2018. Two Rab GTPases play different roles in conidiation, trap formation, stress resistance, and virulence in the nematode-trapping fungus *Arthrobotrys oligospora*. Appl Microbiol Biotechnol 102:4601–4613. https://doi.org/10.1007/s00253-018-8929-1
64. Bai N, Xie M, Liu Q, Wang W, Liu Y, Yang J. 2023. AoSte12 is required for mycelial development, conidiation, trap morphogenesis, and secondary metabolism by regulating hyphal fusion in nematode-trapping fungus *Arthrobotrys Oligospora*. Microbiol Spectr 11:e0395722. https://doi.org/10.1128/spectrum.03957-22
65. Tamura K, Peterson D, Peterson N, Stecher G, Nei M, Kumar S. 2011. Mega5: molecular evolutionary genetics analysis using maximum likelihood, evolutionary distance, and maximum parsimony methods. Mol Biol Evol 28:2731–2739. https://doi.org/10.1093/molbev/msr121
66. Tunlid A, Ahman J, Oliver RP. 1999. Transformation of the nematode-trapping fungus *Arthrobotrys oligospora*. FEMS Microbiol Lett 173:111–116. https://doi.org/10.1111/j.1574-6968.1999.tb13491.x
67. Colot HV, Park G, Turner GE, Ringelberg C, Crew CM, Litvinkova L, Weiss RL, Borkovich KA, Dunlap JC. 2006. A high-throughput gene knockout procedure for neurospora reveals functions for multiple transcription factors. Proc Natl Acad Sci U S A 103:10352–10357. https://doi.org/10.1073/pnas.0601456103
68. Jiang KX, Liu QQ, Bai N, Zhu MC, Zhang KQ, Yang JK. 2022. AoSsk1, a response regulator required for mycelial growth and development, stress responses, trap formation, and the secondary metabolism in *Arthrobotrys oligospora*. J Fungi (Basel) 8:260. https://doi.org/10.3390/jof8030260
69. Zhu MC, Zhao N, Liu YK, Li XM, Zhen ZY, Zheng YQ, Zhang KQ, Yang JK. 2022. The cAMP-PKA signalling pathway regulates hyphal growth, conidiation, trap morphogenesis, stress tolerance, and autophagy in *Arthrobotrys oligospora*. Environ Microbiol 24:6524–6538. https://doi.org/10.1111/1462-2920.16253
70. Yang J, Wang W, Liu Y, Xie M, Yang J. 2023. The MADS-box transcription factor AoRlmA is involved in the regulation of Mycelium development, conidiation, cell-wall integrity, stress response, and trap formation of *Arthrobotrys oligospora*. Microbiol Res 268:127299. https://doi.org/10.1016/j.micres.2022.127299
71. Wang W, Zhao Y, Bai N, Zhang K-Q, Yang J, Ianiri G. 2022. AMPK is involved in regulating the utilization of carbon sources, conidiation, pathogenicity, and stress response of the nematode-trapping fungus *Arthrobotrys Oligospora*. Microbiol Spectr 10. https://doi.org/10.1128/spectrum.02225-22
72. Liu J, Wang ZK, Sun HH, Ying SH, Feng MG. 2017. Characterization of the Hog1 MAPK pathway in the Entomopathogenic fungus *Beauveria bassiana*. Environ Microbiol 19:1808–1821. https://doi.org/10.1111/1462-2920.13671
73. Pang MY, Lin HY, Hou J, Feng MG, Ying SH. 2022. Different contributions of the peroxisomal import protein Pex5 and Pex7 to development, stress response and virulence of insect fungal pathogen *Beauveria bassiana*. J Appl Microbiol 132:509–519. https://doi.org/10.1111/jam.15216
74. Madamanchi NR, Runge MS. 2001. Western blotting. Methods Mol Med 51:245–256. https://doi.org/10.1385/1-59259-087-X:245
75. Livak KJ, Schmittgen TD. 2001. Analysis of relative gene expression data using real-time quantitative PCR and the $2^{-\Delta\delta CT}$ method. Methods 25:402–408. https://doi.org/10.1006/meth.2001.1262
76. Dey B, Thukral S, Krishnan S, Chakrobarty M, Gupta S, Manghani C, Rani V. 2012. DNA-protein interactions: methods for detection and analysis. Mol Cell Biochem 365:279–299. https://doi.org/10.1007/s11010-012-1269-z